UNIVERSIDADE DE SÃO PAULO
INSTITUTO DE FÍSICA DE SÃO CARLOS

Bruno Nicolau Santos

Analysis of narrow-line magneto-optical traps through stochastic simulation

São Carlos

2022

Bruno Nicolau Santos

Analysis of narrow-line magneto-optical traps through stochastic simulation

Dissertation presented to the Graduate Program in Physics at the Instituto de Física de São Carlos da Universidade de São Paulo, to obtain the degree of Master in Science.

Concentration area: Applied Physics

Advisor: Prof. Dr. Emanuel Alves de Lima Henn

Original version

São Carlos

2022

List of Figures

Contents

1 Introduction

The deep understanding of light-matter interaction brought several scientific possibilities such as improvements in the atom interferometry (1), accurate spectroscopic methods (2), and control of ultracold atoms. The Nobel Prize in Physics of 1997 was awarded jointly to Steven Chu (3), Claude Cohen-Tannoudji (4), and William D. Phillips (5) for developing methods to cool and trap atoms with laser light, also known as laser cooling (6). This achievement has enabled modern technologies, including accurate atomic clocks (7), qubits for quantum computing (8), and quantum sensors (9). Laser cooling also allowed the experimental confirmation of the Bose-Einstein condensation (BEC), motivating the Nobel Prize of Physics in 2001 (10, 11).

The workhorse of laser cooling is the magneto-optical trap (MOT) (12), a technique to trap and cool a dilute atomic gas until temperatures in a range of μK. A standard MOT consists of three pairs of counter-propagating laser beams mutually orthogonal and a magnetic quadrupole field. Briefly, the atoms scatter photons from the laser light through atomic transitions, which cause momentum exchanges. The average momentum exchange yields a trapping and drag force on the atoms (MOT force), whereas its fluctuations determine temperature. The frequency of these random scatterings increases with the atomic linewidth and defines the magnitude of both MOT force and fluctuations. Hence, MOTs operating with narrow transitions reach lower temperatures at the cost of trapping efficiency. When the linewidth is comparable to the photonic recoil, we have the narrow line magneto-optical trap (nMOT) (13–15).

The current MOT theories based upon Doppler cooling are rather limited to predict quantities such as temperature (16) and atomic cloud size (17). In many experiments, there is either the absence of theoretical predictions or the necessity of adjustable scaling factors (18). Furthermore, most of these theories are restricted to an unfeasible one-dimensional MOT (6, 19). The difficulty arises from the three-dimensional laser beams arrangement in the presence of a magnetic quadrupole field. There are few papers devoted to develop a 3D MOT model (20), all of them with strong limitations. The case of nMOTs is even more delicate since gravity can be comparable with the optical forces and then must be included. Therefore, it is evident that a computational approach to predict MOT features is appropriate and often required (21–23).

In this thesis, we focus perform a deep analysis of the atom dynamics in nMOTs through a stochastic simulation proposal. Our model relies on sampling ensembles of random atomic trajectories as a discrete stochastic process, more precisely as a Markov chain. To validate the model, we simulate standard six-beam nMOTs of dysprosium and strontium, obtaining results in agreement with experimental measurements. Then we

analyze the nuances of the stochastic dynamics in nMOTs based upon simulated data.

1.1 The thesis

In the framework of this thesis, we execute a deep study of atom-light interactions and stochastic processes aiming to understand the atom dynamics from both optical forces and photon scattering (Markovian process) perspectives. The radiation pressure force is the base of the Doppler cooling theory, whereas the stochastic dynamics theory is essential to computationally approach the atoms dynamics and then infer experimental quantities.

Firstly, we investigate the basic concepts of atom-light interaction through the Einstein rate equations. Although this approach is proper to attend an elementary understanding, it does not contemplate coherent effects such as Rabi oscillations and the nature of line broadening mechanisms. To take these phenomena into account, we introduce the density operator formalism, treating the atom-light interaction semiclassically. Afterwards, we introduce both radiation pressure force and gradient dipole force, also known as optical forces. Finally, we verify the conditions to occur a transition between electronic states.

Study of magneto-optical traps and the limit of narrow-line

Study of stochastic dynamics in nMOTs

Comments about results

2 Atom-light interaction

In this chapter, we review several aspects of atom-light interaction (24) to properly approach the stochastic atomic dynamics in magneto-optical traps. First of all, we shall explore the basic concepts through **the phenomenological Einstein rate equations** (25), a "semi-quantum" model where atoms absorb and emit light at a defined rate. Afterwards, we invoke the quantum mechanics apparatus through the **density operator** and the **master equation** (26) to analyze coherence effects and line broadening mechanisms. We minutely approach the case of a two-level atom interacting with a monochromatic radiation through the semiclassical approach. Finally, we brief discuss conditions in which electric dipole transitions are allowed.

2.1 Rate equations model

A simple approach to introduce the essential aspects of atom-light interaction was proposed by Einstein in 1917. Although this theory does not take coherent effects into account, it is justified within the quantum mechanics framework in appropriate limits. Einstein assumed discrete energy levels for both atom and light. In this context, the electromagnetic radiation is composed of packets of energy $\hbar\omega$ and momentum $\hbar\omega/c$ known as photons, where ω is the angular frequency, $\hbar = h/2\pi$ is the reduced Planck constant, and c is the speed of light. Einstein also postulated phenomenological rate equations to describe two-level atomic transitions due to the absorption and emission of photons. Let us consider a two-level transition where the energy difference between the upper and lower level is $\hbar\omega_0$, and an electromagnetic radiation with spectral energy density $u(\omega)$. In Figure 1, we illustrated the three possible transitions involving absorption and emission of photons.

Let us consider a dilute atomic gas with number density $n_1(t)$ of atoms in the lower level and number density $n_2(t)$ of atoms in the upper level after a period of time t. The Einstein rate equations express the time evolution of n_1 and n_2 so that

$$\frac{dn_1}{dt} = -\frac{dn_2}{dt} = -B_{12}u(\omega_0)n_1 + B_{21}u(\omega_0)n_2 + An_2, \tag{2.1}$$

where $B_{12}u(\omega_0)$, $B_{21}u(\omega_0)$, and A are phenomenological rates associated with the stimulated absorption, stimulated emission and spontaneous emission respectively. The rates associated with stimulated processes are proportional to the spectral density energy and therefore theses processes only happen in the presence of a light field.

Figure 1 – Optical two-level transitions

(a) **Stimulated absorption** (b) **Stimulated emission** (c) **Spontaneous emission**
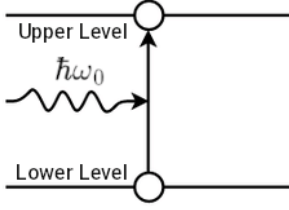
An atom in the lower level goes into the upper level absorbing a photon with energy $\hbar\omega_0$ from a light field with $u(\omega_0) > 0$.
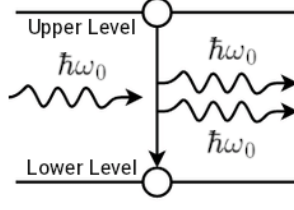
An atom in the upper level decays into the lower level in the presence of a light field with $u(\omega_0) > 0$, emitting a photon with energy $\hbar\omega_0$ similar to the photons in the light field.
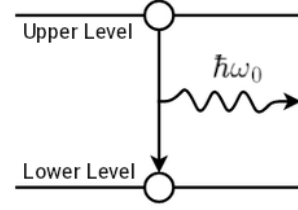
An atom in the upper level emits an isotropic photon with energy $\hbar\omega_0$ spontaneously, decaying into the lower level.

Source: Author

2.1.1   Relation between the Einstein coefficients

A dilute atomic gas at temperature T in thermal equilibrium establishes a steady state in which n_1 and n_2 are constants of time $(d_t n_1 = -d_t n_2 = 0)$. In this condition, from equation (2.1), the spectral energy density is

$$u(\omega_0) = \frac{A}{(n_1/n_2)B_{12} - B_{21}}. \tag{2.2}$$

Considering a fixed number of atoms $n = n_1 + n_2$, the system are represented by the canonical ensemble and then the ratio n_1/n_2 is associated with the Boltzmann distribution so that

$$\frac{n_1}{n_2} = \frac{g_1}{g_2} \exp\left\{-\frac{\hbar\omega_0}{k_B T}\right\}, \tag{2.3}$$

where g_1 and g_2 are the degeneracies of the lower and upper level, respectively, and k_B is the Boltzmann constant. Einstein evaluated atoms in a region of black body radiation, in which the spectral energy density of the light is consistent with the Planck distribution law given by

$$u(\omega_0) = \frac{\hbar\omega_0^3}{\pi^2 c^3} \frac{1}{e^{\hbar\omega_0/k_B T} - 1}. \tag{2.4}$$

Comparing (2.2), (2.3), and (2.4), we obtain

$$B \equiv B_{21} = \frac{g_1}{g_2} B_{12} \tag{2.5}$$

and

$$A = \frac{\hbar\omega_0^3}{\pi^2 c^3} B. \tag{2.6}$$

The Einstein coefficients are properties of the atoms. Thereby the equations (2.6) and (2.5) are valid for any electromagnetic radiation, from narrow bandwidth radiation to broadband light. If we know one of the three rate coefficients, we can always determine the other two.

It is worthwhile to compare the spontaneous emission rate A to the stimulated emission rate $Bu(\omega_0)$ considering the equations (2.4) and (2.6) so that

$$\frac{A}{Bu(\omega_0)} = e^{\hbar\omega_0/k_B T} - 1. \tag{2.7}$$

Spontaneous emission dominates for high frequencies (visible, UV, X-ray), $\hbar\omega_0 \gg k_B T$, but stimulated emission is more relevant for small frequencies (far IR, microwaves, radio waves).

2.1.2 Probabilistic analysis for single atoms

Previously, we consider the effect of the Einstein equations on an atomic sample. In this section, we shall analyze the effect of those equations on a single atom through the probability $P(t)$ of finding an atom in the upper level[1] after a period t,

$$P(t) = \frac{n_2}{n_1 + n_2} = \frac{n_2(t)}{n}. \tag{2.8}$$

From now on, for simplicity, we shall consider non-degenerate atomic transitions ($g_1 = g_2 = 1$). We also shall call the lower level as *ground state* and the upper level as *excited state*. The probability distribution $\rho(t)$ of finding an atom in the excited state between the instants t and $t + dt$ is given by

$$\rho(t) = \frac{dP}{dt} = (1 - 2P)Bu(\omega_0) - AP, \tag{2.9}$$

where we consider (2.1), (2.8), and $1 - P = n_1/n$.

Let us analyze a system only subject to spontaneous emission, assuming an atom in the absence of light ($u(\omega) = 0$) initially in the excited state ($P(0) = 1$). From (2.9), we obtain

$$P(t) = e^{-At} \Rightarrow \rho(t) = Ae^{-At} \tag{2.10}$$

The equation (2.10) indicates an exponential decay, which means an atom in the excited state certainly goes into the ground state after a long period ($P(t) \longrightarrow 0$). Therefore, we can interpret A as a *relaxation rate*. The average time τ in which an atom remains in the excited state, also known as *lifetime*, is given by

$$\tau = \int_0^\infty t\rho(t)dt = \int_0^\infty Ate^{-At}dt = \frac{1}{A} \Rightarrow A = \frac{1}{\tau}. \tag{2.11}$$

In contrast, we can analyze the effect of stimulated processes considering $Bu(\omega_0) \gg A$. Let us assume an atom initially in the ground state ($P(0) = 0$). From equation (2.9), we obtain

$$P(t) = \frac{1 - e^{-\alpha t}}{2} \tag{2.12}$$

---

[1] Analogously, we can define the probability of finding an atom in the lower level.

where $\alpha \equiv 2Bu(\omega_0)$ is the rate in which the radiation raises (or "pumps") atoms into the excited state due to stimulated process, also known as *pumping rate*. The equation (2.12) shows that the strong driving of a transition leads to its *saturation* $(P(t) \longrightarrow 1/2)$. In other words, the atomic ensemble goes into complete transparency.

Finally, let us assume an atom initially in the ground state subjected to the effect of both stimulated and spontaneous processes. In this situation, the solution of (2.9) is

$$P(t) = \frac{1/2}{1 + A/\alpha}(1 - e^{-(A+\alpha)t}) \tag{2.13}$$

The equation (2.13) also indicates a saturation so that

$$\lim_{t \to \infty} P(t) = \frac{1/2}{1 + A/\alpha}. \tag{2.14}$$

In the limits $A \gg \alpha$ and $A \ll \alpha$, we obtain $P(t) \longrightarrow 0$ and $P(t) \longrightarrow 1/2$, respectively. These results are expected from the previous analysis.

2.1.3 Spectral broadening

In the previous section, we assume that the emitted and absorbed photons have a single frequency ω_0. In this case, the probability to absorb or emit a photon is a sharp line centered at $\omega = \omega_0$ as illustrated in figure 2a. However, in real situations, atoms can absorb and emit photons in a range of frequencies due to **line-broadening mechanisms** (section 2.3.8), which is illustrated in figure 2b.

Figure 2 – Spectral broadening

(a) Sharp spectral line

(b) Broadened spectral line
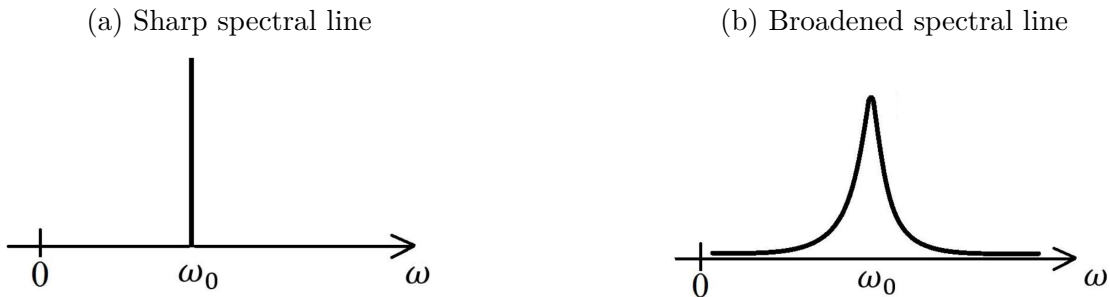
Absorption or emission spectrum without line-broadening mechanisms so that we can assume the line shape $g(\omega) = \delta(\omega - \omega_0)$.

Absorption or emission spectrum taking line-broadening mechanisms into account.

Source: (27)

We can take these mechanisms into account by introducing the normalized function g called **line shape function**. This function can be understood as the probability of absorbing or emitting a photon with frequency between ω and $\omega + d\omega$. A common g

function in atomic spectroscopy is the *Lorentzian*[2] (Cauchy distribution) given by

$$g(\omega) = \frac{\Gamma'}{2\pi} \frac{1}{(\omega - \omega_0)^2 + (\Gamma'/2)^2} \quad \text{or} \quad g(\Delta) = \frac{\Gamma'}{2\pi} \frac{1}{\Delta^2 + (\Gamma'/2)^2}, \tag{2.15}$$

where $\Delta = \omega - \omega_0$ is the **detuning** and Γ' is the full width at half maximum (FWHM) also known as **spectral linewidth**. The main spectral linewidth is $\Gamma' = A$, which is related to the energy-time uncertainty principle. Thus,

$$g(\omega) = \frac{A}{2\pi} \frac{1}{(\omega - \omega_0)^2 + (A/2)^2} \quad \text{or} \quad g(\Delta) = \frac{A}{2\pi} \frac{1}{\Delta^2 + (A/2)^2}. \tag{2.16}$$

The probability distribution of finding an atom in the excited state taking the line shape function into account is given by

$$\rho(t) = (1 - 2P)B \int_0^\infty u(\omega)g(\omega)d\omega - AP. \tag{2.17}$$

For a broadband electromagnetic field, which means $u(\omega)$ much broader than $g(\omega)$, the equations (2.17) and (2.9) are equivalent because

$$\int_0^\infty u(\omega)g(\omega)d\omega \simeq u(\omega_0) \int_0^\infty g(\omega)d\omega = u(\omega_0). \tag{2.18}$$

2.1.4 Monochromatic light field

Let us consider a monochromatic electromagnetic field with frequency ω interacting with an atom initially in the ground state. In the case, the spectral intensity $I(\omega)$ and the spectral density energy $u(\omega)$ of the light field is $I(\omega') = cu(\omega') = I_0\delta(\omega' - \omega)$, where I_0 is the total intensity and $\delta(x)$ is the Dirac delta. Thus,

$$\int_0^\infty u(\omega')g(\omega')d\omega' = \frac{I_0}{c} \int_0^\infty g(\omega')\delta(\omega' - \omega)d\omega' = \frac{I_0}{c}g(\omega). \tag{2.19}$$

From equation (2.17) and (2.19), we obtain

$$\rho(t) = (1 - 2P)\frac{\alpha(\omega)}{2} - AP, \tag{2.20}$$

where $\alpha(\omega) = 2B(I_0/c)g(\omega)$ is the **pumping rate**. The stationary solution of (2.20) is given by

$$P(t) = \frac{1/2}{1 + A/\alpha(\omega)} = \frac{1}{2}\frac{s(\omega)}{1 + s(\omega)}, \tag{2.21}$$

where $s(\omega) = \alpha(\omega)/A$ is the **saturation parameter**, which defines the balance between pumping and relaxation. From equation (2.6), we have

$$s(\omega) = \frac{2\pi^2 c^2}{\hbar\omega_0^3}I_0 g(\omega) = \frac{2\lambda_0^3}{hc}I_0 g(\omega) = \frac{I_0}{I_s}\frac{g(\omega)}{g(\omega_0)}, \quad \text{where} \quad I_s \equiv \frac{\hbar\omega_0^3}{2\pi^2 c^2 g(\omega_0)}. \tag{2.22}$$

The intensity I_s is called **saturation intensity**. When $s(\omega) \gg 1$, stimulated processes are more significant than spontaneous emission, implying the saturation $P \longrightarrow 1/2$. When $s(\omega) \ll 1$, relaxation processes are predominant. In this case, the atom will certainly decay to the ground state, $P \longrightarrow 0$.

---

[2]   Some authors define this distribution as a function of the frequency ν instead of the angular frequency $\omega = 2\pi\nu$.

2.1.5 Absorption cross section

Figure 3 – Absorption Cross Section
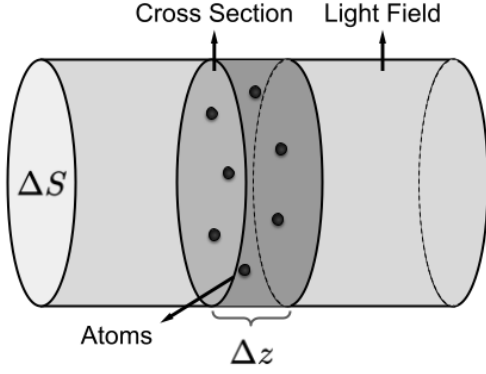
Dilute atomic gas interacting with a electromagnetic radiation in a slab of thickness Δz and volume $\Delta S \Delta z$.
Source: Author

In atomic spectroscopic, it is common to analyze the attenuated or amplified light beam which passes through an atomic medium (28–30). Let us consider an electromagnetic beam with total spectral intensity $I(\omega, z)$ propagating in the z-direction. This radiation passes through an atomic ensemble with n_1 atoms per volume in the ground state and n_2 atoms per volume in the excited state (figure 3), being attenuated or amplified in each slab of thickness Δz due to stimulated absorption. Its spectral intensity will be reduced by a fraction of $n_1\sigma(\omega)\Delta z$, where $\sigma(\omega)$, known as **absorption cross-section**[3], is related to the probability that an atom will absorb an photon with angular frequency between ω and $\omega + d\omega$ from the light field on the section where this light passes on. Therefore, the lost spectral intensity is given $\Delta I/I = -N\sigma\Delta z$ and then

$$\frac{dI}{dz}(\omega, z) = -n_1\sigma(\omega)I(\omega, z). \tag{2.23}$$

Besides the light attenuation due to stimulated absorption, there are also gain due to stimulated emission. Spontaneous emission does not contribute to the gain since the emitted light is isotropic. In this case, the light field will be amplified in each slab, increasing its intensity by a fraction of $n_2\sigma(\omega)\Delta z$. Here, the quantity σ gives the probability of emitting light stimulately. The absorption cross-section and the emission cross-section are the same since the absorption rate equals the emission rate ($B_{12} = B_{21}$ when $g_1 = g_2$). Therefore, the light gain is given by

$$\frac{dI}{dz}(\omega, z) = n_2\sigma(\omega)I(\omega, z). \tag{2.24}$$

From equations (2.23) and (2.24), we obtain

$$\frac{dI}{dz}(\omega, z) = -(n_1 - n_2)\sigma(\omega)I(\omega, z) \tag{2.25}$$

where $(dI/dz)\Delta S \Delta z$ is equivalent to the net spectral power (power per unit of frequency) gained or lost by the radiation in a slab of thickness Δz due to stimulated processes[4]. It is convenient to define a **net absorption cross-section** as

$$\sigma_{abs}(\omega) = \frac{n_1 - n_2}{n}\sigma(\omega) = (1 - 2P)\sigma(\omega), \tag{2.26}$$

---

[3]   The absorption cross-section is expressed in units of area
[4]   Spontaneous emitted light does not come back to the radiation field, since it is isotropic.

where $n = n_1 + n_2$ is the total density number and P is the probability of finding an atom in the excited state. This cross-section is associated with the probability of an atom attenuating or amplifying an incident light due to stimulated processes. Solving the differential equation (2.25), we obtain

$$I(\omega, z) = e^{-n\sigma_{abs}(\omega)t}I(\omega, 0), \tag{2.27}$$

In the regime of weak excitation such that $n_2 \ll n_1$, the total number density is approximately the number density of the atoms in the ground state $n \simeq n_1$ and then $\sigma_{abs}(\omega) \simeq \sigma(\omega)$.

Let us assume a *monochromatic* radiation whose frequency is ω such that $I(\omega', z) = I_0(z)\delta(\omega' - \omega)$ and $u(\omega', z) = I(\omega', z)/c$. In this case, integrating equation (2.25) over all frequencies, we obtain the total power per unit of volume gained or lost by the radiation

$$\frac{dI_0}{dz}(z) = -n\sigma_{abs}(\omega)I_0(z) \quad \Rightarrow \quad I_0(z) = I_0(0)e^{-n\sigma_{abs}(\omega)z}. \tag{2.28}$$

In the steady state, (dI_0/dz) equals the total power per unit of volume lost by spontaneous emission. Then, from equation (2.28), we have

$$n\sigma_{abs}(\omega)I_0 = An_2\hbar \int_0^\infty \omega g(\omega)d\omega. \tag{2.29}$$

Since ω_0 is much greater than the FWHM of $g(\omega)^5$, thus

$$\int_0^\infty \omega g(\omega)d\omega \simeq \omega_0. \tag{2.30}$$

Then, from equation (2.29), we have

$$n\sigma_{abs}(\omega)I_0 = An_2\hbar\omega_0 \quad \Rightarrow \quad \sigma_{abs}(\omega) = \frac{\hbar\omega_0}{I_0}AP, \tag{2.31}$$

where $P = n_2/n$. Therefore, in the steady state, the *net absorption cross-section* can be understood as an area on which the photon flux of the incident beam passes through times the rate ΓP at which an atom scatters photons by spontaneous emission, i.e. the decay rate Γ times the probability of finding an atom in the excited state. From equations (2.21), (2.22), and (2.31), we obtain

$$\sigma(\omega) = \frac{\hbar\omega_0}{I_0}\frac{A}{2}s(\omega) = \overbrace{\frac{\hbar\omega_0}{I_s}\frac{A}{2}}^{\sigma_0}\frac{g(\omega)}{g(\omega_0)} = \sigma_0\frac{g(\omega)}{g(\omega_0)} \quad \text{and} \tag{2.32}$$

$$\sigma_{abs}(\omega) = \frac{\hbar\omega_0}{I_0}\frac{A}{2}\frac{s(\omega)}{1 + s(\omega)} = \sigma(\omega)\frac{1}{1 + s(\omega)}, \tag{2.33}$$

where $\sigma_0 \equiv \sigma(\omega_0)$ is the *resonant absorption cross-section* which only depends on the properties of the atom (I_s, ω_0, and A).

---

[5] The line shape function must be normalized over 0 to ∞, which demands that the peak frequency ω_0 of $g(\omega)$ must be much greater than its FWHM.

2.2 Semiclassical approach

In the previous section, we consider phenomenological rate equations to study two-level atomic transitions. This approach does not contemplate coherence effects nor a fundamental understanding of line broadening mechanisms. In a first attempt, we can take the coherence effects into account assuming the interaction between a classical light field (electromagnetic waves) and an atom whose internal states are described by a quantum state vector $|\psi\rangle$. Indeed, this is a proper treatment as long as we are only interested in stimulated processes. However, spontaneous emission comes from the interaction between atom and the vacuum modes of the quantized electromagnetic field, an incoherent relaxation process. Therefore, a single state vector is not sufficient to analyze an atom under both stimulated and spontaneous processes since such system is under decoherence. A proper description comes through the density operator, which describes a statistical mixture of quantum states. This approach allows us to study the system time evolution taking both coherent and incoherent processes into account through a master equation. In this section, we shall introduce the density operator formalism to investigate atom-light interaction.

2.2.1 The density operator

The density operator represents an **ensemble** of identical systems in different quantum states. Let us consider a system which can be found in a quantum state $|\psi_k\rangle$ with probability P_k. This system is represented by the following density operator

$$\hat{\rho} \equiv \sum_k P_k |\psi_k\rangle\langle\psi_k| \quad \text{so that} \quad \sum_k P_k = 1. \tag{2.34}$$

When the system is described by a single state vector $|\psi\rangle$, which means $\hat{\rho} = |\psi\rangle\langle\psi|$, it is said to be in a **pure state**, otherwise it is said to be in a **mixed state**.

Let us consider the orthonormal basis $\{|n\rangle : n \in \{1, 2, \cdots, N\}\}$ on which it is possible to represent the states $\{|\psi_k\rangle\}$ and the density operator $\hat{\rho}$ as

$$|\psi_k\rangle = \sum_{n=1}^{N} |c_{k,n}|e^{\phi_{k,n}} |n\rangle, \quad \hat{\rho} = \begin{bmatrix} \rho_{1,1} & \cdots & \rho_{1,N} \\ \vdots & \ddots & \vdots \\ \rho_{N,1} & \cdots & \rho_{N,N} \end{bmatrix}, \tag{2.35}$$

$$\text{where} \quad \rho_{m,n} = \langle m|\hat{\rho}|n\rangle \quad \text{(matrix elements)}, \tag{2.36}$$

being ρ the **density matrix** and $c_{k,n} = |c_{k,n}|e^{\phi_{k,n}}$. From now on, we shall assuming the abuse of notation $\hat{\rho} = \rho$ in order to make the definion of a density operator easy by using its matrix represantion. The probability of finding a state $|n\rangle$ in a given state vector $|\psi_k\rangle$ is $P_k|c_{k,n}|^2$. Then the probability of finding the state $|n\rangle$ in any state vector is

$$\sum_k P_k|c_{k,n}|^2 = \sum_k P_k \underbrace{\langle n|\psi_k\rangle}_{c_{k,n}} \underbrace{\langle\psi_k|n\rangle}_{c_{k,n}^*} = \langle n| \left(\sum_k P_k |\psi_k\rangle\langle\psi_k| \right) |n\rangle = \langle n|\hat{\rho}|n\rangle = \rho_{n,n}. \tag{2.37}$$

Therefore, the diagonal terms, also referred as **populations**, give the probability of measuring the system in some state $|n\rangle$, which implies

$$\text{Tr}[\rho] = \sum_{n=1}^{N} \langle n|\hat{\rho}|n\rangle = \sum_{n=1}^{N} \rho_{n,n} = 1, \qquad (2.38)$$

where $Tr[\hat{\rho}]$ is the **trace** of the operator $\hat{\rho}$. This operation is independent of the basis since it is invariant with respect to any unitary transformation. Moreover, the trace is also invariant under cyclic permutation of the product so that

$$\text{Tr}\left[\hat{A}\hat{B}\hat{C}\right] = \text{Tr}\left[\hat{B}\hat{C}\hat{A}\right] = \text{Tr}\left[\hat{C}\hat{A}\hat{B}\right]. \qquad (2.39)$$

The off-diagonal terms are called **coherences**. They give information about the relative phase of different components. Let us consider a pure state so that

$$\rho_{m,n} = \langle m| \left(|\psi\rangle\langle\psi|\right) |n\rangle = \langle m| \left(\sum_p |c_p|e^{i\phi_p} |p\rangle\right) \left(\sum_q |c_q|e^{-i\phi_q} \langle q|\right) |n\rangle \qquad (2.40)$$

$$= \sum_{p,q} |c_p c_q| e^{i(\phi_p - \phi_q)} \langle m|p\rangle \langle q|n\rangle = |c_m c_n| e^{i(\phi_m - \phi_n)} \qquad (2.41)$$

For mixed systems, the coherences will be the sum of complex numbers corresponding to different states $|\psi_k\rangle$. Furthermore, it is possible to check whether a system is pure or mixed evaluating the quantity $\text{Tr}[\hat{\rho}^2]$. For a pure state $\hat{\rho}_{pure} = |\psi\rangle\langle\psi|$, we have

$$\hat{\rho}_{pure}^2 = |\psi\rangle \langle\psi|\psi\rangle \langle\psi| = |\psi\rangle\langle\psi| = \hat{\rho}_{pure} \Rightarrow \text{Tr}\left[\hat{\rho}_{pure}^2\right] = \text{Tr}[\hat{\rho}_{pure}] = 1. \qquad (2.42)$$

Indeed, $\hat{\rho}_{pure}^n = \hat{\rho}_{pure}$ for any pure state, being n a non-negative integer. To study the case of a mixed state defined by the density operator $\hat{\rho}_{mixed}$, let us assume a basis where the matrix ρ_{mixed} is diagonal so that

$$\text{Tr}\left[\rho_{mixed}^2\right] = \sum_n (\rho_{n,n})^2 \leq \sum_n \rho_{n,n} = 1, \qquad (2.43)$$

since $0 \leq \rho_{n,n} \leq 1$. A diagonal pure state has only a single non-zero element, whereas a diagonal mixed state necessarily has more then one non-zero element. Hence, being the trace operation independent of the basis, for a mixed state we always have

$$\text{Tr}\left[\hat{\rho}_{mixed}^2\right] < 1. \qquad (2.44)$$

We can also compute expectation values using the trace operation. Let us consider an observable $\hat{A}$ whose matrix elements are $A_{m,n} = \langle m|\hat{A}|n\rangle$. The expectation value $\langle\hat{A}\rangle$ is expressed by

$$\langle\hat{A}\rangle = \sum_k P_k \langle\psi_k|\hat{A}|\psi_k\rangle. \qquad (2.45)$$

On the other side,

$$\hat{\rho}\hat{A} = \sum_k P_k \,|\psi_k\rangle\langle\psi_k|\,\hat{A} \Rightarrow \langle n|\hat{\rho}\hat{A}|n\rangle = \sum_k P_k \,\langle\psi_k|\hat{A}|n\rangle\,\langle n|\psi_k\rangle \Rightarrow \tag{2.46}$$

$$\Rightarrow \mathrm{Tr}\!\left[\hat{\rho}\hat{A}\right] = \sum_n \langle n|\hat{\rho}\hat{A}|n\rangle = \sum_k P_k \,\langle\psi_k|\,\hat{A}\underbrace{\left(\sum_{n=1}^N |n\rangle\langle n|\right)}_{\mathbb{I}}|\psi_k\rangle = \sum_k P_k \,\langle\psi_k|\hat{A}|\psi_k\rangle \tag{2.47}$$

$$\therefore \mathrm{Tr}\!\left[\hat{\rho}\hat{A}\right] = \sum_k P_k \,\langle\psi_k|\hat{A}|\psi_k\rangle = \langle\hat{A}\rangle. \tag{2.48}$$

Therefore, the ensemble average of any observable $\hat{A}$ can be calculated from the diagonal elements of the operator matrix $\hat{\rho}\hat{A}$.

The density operator formalism is also great to manage **composite system**. Let us consider a system A defined by the density operator $\hat{\rho}_A$ and the Hilbert space $\mathcal{H}_A$, and a system B represented by the density operator $\hat{\rho}_B$ and the Hilbert space $\mathcal{H}_B$. The total system, which take A and B into account, is described by the density operator $\hat{\rho}_{AB}$ and the Hilbert Space $\mathcal{H}_A \otimes \mathcal{H}_B$. The operator $\hat{\rho_A}$ and $\hat{\rho_B}$ can be seen as **reduced density matrices**, which can be derived from $\hat{\rho}_{AB}$ through the **partial trace operation**,

$$\hat{\rho}_A = \mathrm{Tr}_B[\hat{\rho}_{AB}] \quad \text{and} \quad \hat{\rho}_B = \mathrm{Tr}_A[\hat{\rho}_{AB}]. \tag{2.49}$$

Let us consider a pure state $|\psi_{AB}\rangle$ of both system A and B given by

$$|\psi_{AB}\rangle = \sum_{m,n} c_{m,n}\,|m\rangle \otimes |n\rangle, \quad \text{where} \quad \sum_{m,n}|c_{m,n}| = 1. \tag{2.50}$$

If the systems are *independent*, we can associate a state $|\psi_A\rangle = \sum a_m\,|m\rangle$ to the system A and $|\psi_B\rangle = \sum b_n\,|n\rangle$ to the system B so that

$$|\psi_{AB}\rangle = |\psi_A\rangle \otimes |\psi_B\rangle = \left(\sum_m a_m\,|m\rangle\right) \otimes \left(\sum_n b_n\,|n\rangle\right) = \sum_{m,n} a_m b_n\,|m\rangle \otimes |n\rangle. \tag{2.51}$$

From equations (2.50) and (2.51), we obtain $c_{m,n} = a_m b_n$. Then, the density operator $\hat{\rho}_{AB}$ is given by

$$\hat{\rho}_{AB} = |\psi_{AB}\rangle\langle\psi_{AB}| = \sum_{m,n}\sum_{m',n'} a_m a_{m'} b_n b_{n'} \,|m\rangle\langle m'| \otimes |n\rangle\langle n'| =$$

$$= \left(\sum_{m,m'} a_m a'_m \,|m\rangle\langle m'|\right) \otimes \left(\sum_{n,n'} b_n b'_n \,|n\rangle\langle n'|\right) =$$

$$= |\psi_A\rangle\langle\psi_A| \otimes |\psi_B\rangle\langle\psi_B| = \hat{\rho}_a \otimes \hat{\rho}_B. \tag{2.52}$$

Therefore, when two systems A and B are **uncorrelated** or *independent*, we can write the density operator of both systems as a tensor product between the density operator of the system A and the density operator of the system B,

$$\hat{\rho}_{AB} = \hat{\rho}_A \otimes \hat{\rho}_B. \tag{2.53}$$

2.2.2 Two-level system and the Bloch sphere

Let us consider a system composed of only two quantum states $|1\rangle$ and $|2\rangle$, in which $|1\rangle$ is the *ground state* and $|2\rangle$ is the excited state. An arbitrary two-dimensional density operator can be represent as

$$\hat{\rho} = \begin{bmatrix} \rho_{1,1} & \rho_{1,2} \\ \rho_{2,1} & \rho_{2,2} \end{bmatrix}, \tag{2.54}$$

where $\rho_{i,j} = \langle i|\hat{\rho}|j\rangle$. In the previous section 2.2.1, we saw that the diagonal terms represent probabilities so that $\rho_{1,1} + \rho_{2,2} = 1$, being $\rho_{1,1}$ and $\rho_{2,2}$ real values. Also, $\hat{\rho}$ must be hermitian and therefore $\rho_{1,2} = (\rho_{2,1})^*$. The density matrix (2.54) is represented on the basis

$$\left\{ \begin{bmatrix} 1 & 0 \\ 0 & 0 \end{bmatrix}, \begin{bmatrix} 0 & 1 \\ 0 & 0 \end{bmatrix}, \begin{bmatrix} 0 & 0 \\ 1 & 0 \end{bmatrix}, \begin{bmatrix} 0 & 0 \\ 0 & 1 \end{bmatrix} \right\}. \tag{2.55}$$

Another convenient basis is the **Pauli matrices basis**,

$$\left\{ \sigma_x = \begin{bmatrix} 0 & 1 \\ 1 & 0 \end{bmatrix}, \ \sigma_y = \begin{bmatrix} 0 & -i \\ i & 0 \end{bmatrix}, \ \sigma_z = \begin{bmatrix} 1 & 0 \\ 0 & -1 \end{bmatrix}, \ \mathbb{I}_2 = \begin{bmatrix} 1 & 0 \\ 0 & 1 \end{bmatrix} \right\}, \tag{2.56}$$

where σ_x, σ_y, and σ_z are the *Pauli matrices*. An arbitrary density matrix on this basis is written as[6]

$$\hat{\rho} = \frac{1}{2}(\mathbb{I}_2 + \mathbf{a} \cdot \vec{\sigma}) = \frac{1}{2} \begin{bmatrix} 1 + a_3 & a_1 - ia_2 \\ a_1 + ia_2 & 1 - a_3 \end{bmatrix}, \tag{2.57}$$

$$\text{where} \ \ \vec{\sigma} = \begin{bmatrix} \sigma_x \\ \sigma_y \\ \sigma_z \end{bmatrix} \ \ \text{and} \ \ \mathbf{a} = \begin{bmatrix} a_1 \\ a_2 \\ a_3 \end{bmatrix} (\textbf{Bloch vector}). \tag{2.58}$$

In this representation, its eigenvalues are $(1 \pm |\mathbf{a}|)/2$. Since they are probabilities, we must have $0 \leq (1 \pm |\mathbf{a}|)/2 \leq 1 \Rightarrow |\mathbf{a}| \leq 1$. For the same reason, the diagonal terms, and then a_3, must be positive values. Furthermore, $\hat{\rho} = \hat{\rho}^\dagger$, which implies $a_1 = a_1^*$ and $a_2 = a_2^*$. Hence, $\mathbf{a}$ is a real vector. Comparing with the density matrix (2.54), we have $a_3 = \rho_{1,1} - \rho_{2,2} = p$ and $(a_1 + ia_2)/2 = \rho_{2,1} = q$, where p is known as **population inversion** and q is the *coherence*. Then, the Bloch vector and the density matrix can be written as

$$\mathbf{a} = \begin{bmatrix} 2\,\text{Re}[q] \\ 2\,\text{Im}[q] \\ p \end{bmatrix} = \begin{bmatrix} q + q^* \\ i(q^* - q) \\ p \end{bmatrix} \ \ \text{and} \ \ \hat{\rho} = \begin{bmatrix} (1+p)/2 & q^* \\ q & (1-p)/2 \end{bmatrix}. \tag{2.59}$$

Taking the property $|\mathbf{a}| \leq 1$ into account, we can represent the Bloch vector in a ball of unitary radius known as **Bloch sphere** (although it is a ball, not a sphere) illustrated in

---

[6] For an arbitrary operator, we should have four coefficients $[\hat{A}] = a_0\mathbb{I} + a_1\sigma_x + a_2\sigma_y + a_3\sigma_z$. In the case of the density matrix, we must have $a_0 = 1/2$ due to the property $\text{Tr}[\hat{\rho}] = 1$.

figure 4. The axes are given by $x = 2\operatorname{Re}[q]$, $y = 2\operatorname{Im}[q]$, and $z = p$. When $\hat{\rho}$ represent a pure state, we have

$$\operatorname{Tr}\left[\hat{\rho}^2\right] = 1 \Rightarrow \frac{1}{2}(1 + |\mathbf{a}|^2) = 1 \Rightarrow |\mathbf{a}|^2 = 1. \tag{2.60}$$

Therefore, the surface of the Bloch sphere represents all the pure states, whereas the inside corresponds to all the mixed states.

Figure 4 – Bloch sphere.
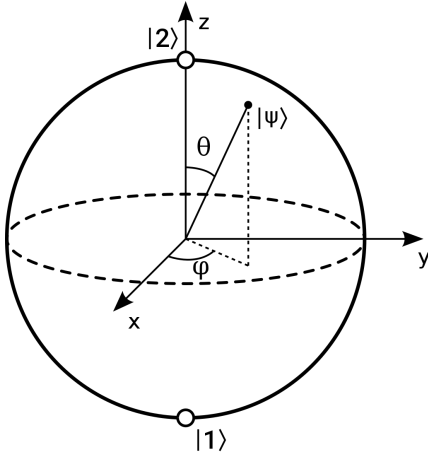
Bloch sphere for a pure state given by $|\psi\rangle = \sin(\theta/2)|1\rangle + e^{i\phi}\cos(\theta/2)|2\rangle$.
Source: Author

Let us consider a pure state $|\psi\rangle = c_1|1\rangle + c_2|2\rangle$. Since a global phase is not measurable, we can assume $|\psi\rangle = c_1|1\rangle + c_2 e^{i\phi}|2\rangle$ where ϕ is the phase difference between $|1\rangle$ and $|2\rangle$, and both c_1 and c_2 are real values. Moreover, $c_1^2 + c_2^2 = 1$, which allows us to associate c_1 and c_2 with a unique value θ considering $c_1 = \sin(\theta/2)$ and $c_2 = \cos(\theta/2)$. Even though the value of θ is not unique to represent c_1 and c_2, the point (θ, ϕ) is unique to represent $|\psi\rangle$. Thus, a density operator $\hat{\rho} = |\psi\rangle\langle\psi|$ of a pure state can be written as

$$\begin{aligned} \hat{\rho} &= \sin^2(\theta/2)|1\rangle\langle 1| + \cos^2(\theta/2)|2\rangle\langle 2| + \\ &+ \frac{1}{2}e^{-i\phi}\sin\theta|1\rangle\langle 2| + \frac{1}{2}e^{i\phi}\sin\theta|2\rangle\langle 1|, \end{aligned} \tag{2.61}$$

$$\hat{\rho} = \begin{bmatrix} \sin^2(\theta/2) & \frac{1}{2}e^{-i\phi}\sin\theta \\ \frac{1}{2}e^{i\phi}\sin\theta & \cos^2(\theta/2) \end{bmatrix}. \tag{2.62}$$

From equations (2.57) and (2.62), we obtain the following Bloch vector

$$\mathbf{a} = (\cos\phi\sin\theta, \sin\phi\sin\theta, \cos\theta), \tag{2.63}$$

in which (ϕ, θ) are *spherical coordinates* represented in figure 4.

2.2.3 Liouville equation

The time evolution of a state vector $|\psi\rangle$ is given by the Schrodinger equation $\hat{H}|\psi\rangle = i\hbar\partial_t|\psi\rangle$, where $\hat{H}$ is the Hamiltonian of the system. Thereby, the time evolution of $\hat{\rho}$ is given by

$$\partial_t\hat{\rho} = \partial_t\left(\sum_k P_k|\psi_k\rangle\langle\psi_k|\right) = \sum_k P_k[(\partial_t|\psi_k\rangle)\langle\psi_k| + |\psi_k\rangle(\partial_t\langle\psi_k|)] = \tag{2.64}$$

$$= \frac{i}{\hbar}\sum_k P_k(|\psi_k\rangle\langle\psi_k|\hat{H} - \hat{H}|\psi_k\rangle\langle\psi_k|) = \hat{\rho}\hat{H} - \hat{H}\hat{\rho} \tag{2.65}$$

Therefore,

$$\partial_t\hat{\rho} = \frac{i}{\hbar}[\hat{\rho}, \hat{H}], \tag{2.66}$$

where the equation (2.66) is called **von Neumann equation** or **Liouville equation**. The commutator itself can be considered as a **superoperator** acting on the density operator,

$$\mathcal{L}\hat{\rho}(t) \equiv -\frac{i}{\hbar}[\hat{H}, \hat{\rho}(t)], \tag{2.67}$$

where $\mathcal{L}$ is known as **Liouville superoperator**. We shall work with a Hamiltonian in the form $\hat{H} = \hat{H}_0 + \hat{V}(t)$, where $\hat{H}_0$ is a time-independent part and $\hat{V}(t)$ is a time-dependent term. In this case, it is convenient to define an unitary transformation given by $\hat{U}(t) = e^{-i\hat{H}_0 t/\hbar}$ so that

$$\hat{\rho}'(t) = \hat{U}^\dagger(t)\hat{\rho}(t)\hat{U}(t). \tag{2.68}$$

Calculating the time derivatives on both sides of (2.68) and assuming (2.66), we obtain

$$\partial_t\hat{\rho}'(t) = -\frac{i}{\hbar}[\hat{V}(t), \hat{\rho}'(t)]. \tag{2.69}$$

The equation (2.69) is the **Liouville equation** in the **interaction picture**, which depends only on the time-dependent part.

The equation (2.66) is valid as long as there are only coherent effects on the system, since these processes are represented by unitary time evolutions[7]. In the context of atom-light interaction when we assume an density operator associated with the atomic internal states, the Liouville equation only describes stimulated absorption and emission. However, spontaneous emission is a predominant process in MOTs, so it is mandatory to take it into account. In order to comply with that, we shall introduce the *master equation* in section 2.2.4.

2.2.4 Master equation

Spontaneous emission comes from a coupling between an open quantum system, described by the density operator $\hat{\rho}_S$, and the environment, represented by the density operator $\hat{\rho}_E$. Moreover, the environment must have far more degrees of freedom than the system. In our case, the system can be understood as the atom and the environment as the vacuum modes of the quantized electromagnetic field. Let us consider a density operator $\hat{\rho}_{SE}$ which represents jointly the system and the environment. Assuming a weak coupling in which the system performs a small perturbation to the environment, we can treat both independently so that

$$\hat{\rho}_{SE} \approx \hat{\rho}_S \otimes \hat{\rho}_E. \tag{2.70}$$

The equation (2.70) is known as the **Born approximation**. At first, both system and environment provoke mutual excitations, getting out of thermal equilibrium. After a while, both will reach equilibrium again through a relaxation process. Let us consider the relaxation times τ_E and τ_S of the environment and the system, respectively. Since the system

---

[7]   An unitary time evolution is associated with a hermitian Hamiltonian so that $\hat{U} = e^{-i\hat{H}t/\hbar}$.

causes small perturbation to the environment but the environment interacts strongly with the system, we can consider $\tau_E \ll \tau_S$. This is known as **Markov approximation**. The equation of motion of $\hat{\rho}_{SE}$ is given by the Liouville equation,

$$i\hbar\partial_t\hat{\rho}_{SE} = [\hat{H}_{SE}, \hat{\rho}_{SE}]. \tag{2.71}$$

Let us consider a multi-level system given by the basis $\{|n\rangle\}$. Taking the Born-Markov approximation into account, it is possible to derive an equation of motion for $\hat{\rho}_S$ tracing out the environment in equation (2.71). The resulting equation (31), known as **master equation** or **Lindblad equation**, is given by

$$\partial_t\hat{\rho}_S = \frac{1}{i\hbar}[\hat{H}_S, \hat{\rho}_S] + \sum_{i,j}\frac{\Gamma_{ij}}{2}(2\hat{\sigma}_{ij}\hat{\rho}_S\hat{\sigma}_{ji} - \{\hat{\sigma}_{ji}\hat{\sigma}_{ij}, \hat{\rho}_S\}) = (\mathcal{L} + \mathcal{L}_{decay})\hat{\rho}_S, \tag{2.72}$$

$$\mathcal{L}_{decay}\hat{\rho} = \sum_{i,j}\frac{\Gamma_{ij}}{2}(2\hat{\sigma}_{ij}\hat{\rho}_S\hat{\sigma}_{ji} - \{\hat{\sigma}_{ji}\hat{\sigma}_{ij}, \hat{\rho}_S\}), \tag{2.73}$$

where $\hat{\sigma}_{ij} = |i\rangle\langle j|$, $\mathcal{L}_{decay}$ is the **Lindblad superoperator**, $\{\hat{A}, \hat{B}\} = \hat{A}\hat{B} + \hat{A}\hat{B}$ is the anticommutator, and $\{\Gamma_{i,j}\}$ are rates, known as *decay rates*, at which both populations and coherences vanish. The operators $\hat{\sigma}_{i,j}$ and $\hat{\sigma}_{j,i} = \hat{\sigma}_{i,j}^\dagger$ can be understood as *lower* and *upper operators* between the states $|i\rangle$ and $|j\rangle$ so that $\hat{\sigma}_{i,j}|j\rangle = |i\rangle$ and $\hat{\sigma}_{j,i}|i\rangle = |j\rangle$. The master equation results in the Liouville equation when $\Gamma_{ij} \longrightarrow 0$, $\forall i, j$. Therefore, the difference between these equations is the decay term expressed by the superoperator $\mathcal{L}_{decay}$ known as **Lindblad superoperator**.

Let us consider the case in which only $\{\Gamma_{i,i} = \Gamma_i\}$ are non-zero. Then, the super-operator $\mathcal{L}_{decay}$ can be written as

$$\mathcal{L}_{decay}\hat{\rho} = -\frac{1}{2}\sum_i\Gamma_i\left(\sum_{j\neq i}\rho_{i,j}|i\rangle\langle j| + \sum_{k\neq i}\rho_{k,i}|k\rangle\langle i|\right), \tag{2.74}$$

where $\rho_{i,j} \equiv \langle i|\hat{\rho}|j\rangle$. From equation (2.74), it is possible to see that only the off-diagonal terms are affected by $\mathcal{L}_{decay}$. Hence, only the coherences decay since they are associated with the off-diagonal terms. This process is known as **pure dephasing**. In the general case when $\Gamma_{i,j} > 0$ for $i \neq j$, the populations also change over time, which is known as **relaxation**. Spontaneous emission is only responsible for *relaxation* terms $\{\Gamma_{i,j}, \ i \neq j, \ i < j\}$, whereas the *pure dephasing* terms $\{\Gamma_i\}$ are associated with **elastic collisions**. Furthermore, $\{\Gamma_i\}$ are the rates at which the atoms collide between each other. We are concerned only with the regime of low temperatures in which collisions are negligible.

2.3 Two-level atom interacting with classical light field

In this section, we deeply study the interaction between a classical monochromatic radiation and a two-level atom through the semiclassical approach presented in section

2.2. We shall explore both coherent effects (*Rabi oscillation*) and line-broadening mechanisms, which are not essentially contemplated by the rate equations model discussed in section 2.1. We also analyze mechanical effects through average forces derived from the *Ehrenfest theorem*. Theses forces, known as **optical forces**, are divided into two: **radiation pressure force** and **gradient dipole force**.

2.3.1   Interaction Hamiltonian

Let us consider a system formed by only two electronic states $\{\ket{1}, \ket{2}\}$[8], each one is a possible state of a valence electron in an atom. This system is well described by the density operator $\hat{\rho}$ given by (2.59). The dynamics of theses states in the absence of a light field is given by the following Hamiltonian

$$\hat{H}_0 = \hbar\omega_1 \ket{1}\bra{1} + \hbar\omega_2 \ket{2}\bra{2} = \hbar\omega_1 \hat{\sigma}\hat{\sigma}^\dagger + \hbar\omega_2 \hat{\sigma}\hat{\sigma}^\dagger, \tag{2.75}$$

where $\hat{\sigma} \equiv \ket{1}\bra{2}$ and $\omega_1 < \omega_2$. The lowest energy state $\ket{1}$ is called *ground state*, whereas the highest energy state $\ket{2}$ is called *excited state*. Since we are only concern with energy differences, we can shift the zero of energy adding $-\hbar\omega_1$ to each energy level so that

$$\hat{H}_0 = \hbar\omega_0 \hat{\sigma}^\dagger\hat{\sigma} = \begin{bmatrix} 0 & 0 \\ 0 & \hbar\omega_0 \end{bmatrix}, \tag{2.76}$$

where $\omega_0 = \omega_2 - \omega_1$ is the **resonant frequency**. The matrix in the equation (2.76) and also further matrix are represented on the basis $\{\ket{1}, \ket{2}\}$. Moreover, we shall assume a monochromatic radiation whose *electric field* $\mathbf{E}$ is given by

$$\mathbf{E}(\mathbf{r}, t) = \frac{\vec{\epsilon}}{2}(E_0 e^{i\mathbf{k}\cdot\mathbf{r} - i\omega t} + E_0^* e^{-(i\mathbf{k}\cdot\mathbf{r} - i\omega t)}), \tag{2.77}$$

where $\vec{\epsilon} = (\vec{\epsilon})^*$ is the *polarization vector*, E_0 is the *complex amplitude*, $\mathbf{k}$ is the *wave vector*, ω is the *angular frequency*, and $\mathbf{r}$ is the *position vector*. The interaction between the electric field $\mathbf{E}$ and the *electric dipole* formed by the valence electron and the atomic nucleus is the major atom-light interaction described by the following Hamiltonian

$$\hat{V} = -\mathbf{d} \cdot \mathbf{E}, \tag{2.78}$$

where $\mathbf{d} = -e\mathbf{r}_e$ is the **dipole operator**, $e \simeq 1.6 \times 10^{-19} C$ is the elementary charge, and $\mathbf{r}_e$ is the valence electron position in the nucleus frame. The typical values of $|\vec{\mu}|$ are around ea_B[9], where $a_B = 0.529\text{Å} = 0.529 \cdot 10^{-10} m$ is the *Bohr radius*. Atoms do not have

---

[8]   Actually, there are many electronic states which can be relevant. However, in many cases, only two states are enough to described the interaction.

[9]   The *debye* (symbol D) is a standard unit measure for electric dipole moment in the atomic and molecular scale, $1D \equiv 10^{-18} statC \cdot cm$. Historically, the debye was defined as the dipole moment of a system composed of two electric charges of opposite sign and equal magnitude $10^{-10} statC \simeq 0.2083 e$ separated by 1Å.

permanent dipole moment due to the parity of the electrons position. Hence, the dipole operator can be written as[10]

$$\mathbf{d} = (\vec{\mu})^*\hat{\sigma} + \vec{\mu}\hat{\sigma}^\dagger, \tag{2.79}$$

where $\vec{\mu} \equiv \langle 2|\mathbf{d}|1\rangle$ is the **transition dipole moment**. When $|\vec{\mu}| = 0$, the transition is said to be **dipole forbidden**. Then, from equations (2.77), (2.157), and (2.78), we obtain the following interaction Hamiltonian

$$\hat{V}(t) = \frac{\hbar}{2}[(\tilde{\Omega}^*(\mathbf{r})e^{-i\omega t} + \Omega^*(\mathbf{r})e^{i\omega t})\hat{\sigma} + (\Omega(\mathbf{r})e^{-i\omega t} + \tilde{\Omega}(\mathbf{r})e^{i\omega t})\hat{\sigma}^\dagger], \tag{2.80}$$

$$\Omega(\mathbf{r}) \equiv -\frac{E_0(\vec{\epsilon}\cdot\vec{\mu})}{\hbar}e^{i\mathbf{k}\cdot\mathbf{r}} \text{ and } \tilde{\Omega}(\mathbf{r}) \equiv -\frac{E_0^*(\vec{\epsilon}\cdot\vec{\mu})}{\hbar}e^{-i\mathbf{k}\cdot\mathbf{r}}, \tag{2.81}$$

where $\Omega(\mathbf{r})$ and $\tilde{\Omega}(\mathbf{r})$ are known as **Rabi frequencies**[11].

2.3.1.1 Dipole approximation

The minimum wavelength of non-ionizing radiation, which is the typical spectral range in laser cooling experiments, is around $100nm = 1000\text{Å}$, whereas the atomic size is around the Bohr radius $a_B \simeq 0.5\text{Å}$. Then, atoms are approximately thousand times smaller than the field spatial variation. Hence, assuming a quasi-static atom, we can neglect the spatial variation of the electromagnetic field in the dynamics of the electronic states. In this case, the Rabi frequency is approximately spatial-independent $\Omega(\mathbf{r}) \simeq \Omega$, which is known as **dipole approximation**.

2.3.1.2 Rotating wave approximation

The typical values of $|\Omega|$ are around MHz, whereas the typical atomic resonant frequencies are around 100THz. Thereby $\hat{V} \sim \hbar|\Omega| \ll \hbar\omega_0$, which allows us to treat the interaction as a perturbation on the system. In the *Dirac picture*, also called *interaction picture*, considering $\hat{U} = e^{-i\hat{H}_0 t/\hbar} = \hat{\sigma}\hat{\sigma}^\dagger + e^{-i\omega_0 t}\hat{\sigma}^\dagger\hat{\sigma}$, we have

$$\tilde{V}(t) = \hat{U}^\dagger\hat{V}\hat{U} = \tilde{V}_{fast}(t) + \tilde{V}_{slow}(t), \tag{2.82}$$

$$\tilde{V}_{fast}(t) = \frac{\hbar}{2}(\tilde{\Omega}^*e^{-i(\omega+\omega_0)t}\hat{\sigma} + \tilde{\Omega}e^{i(\omega+\omega_0)t}\hat{\sigma}^\dagger), \tag{2.83}$$

$$\tilde{V}_{slow}(t) = \frac{\hbar}{2}(\Omega e^{-i\Delta t}\hat{\sigma}^\dagger + \Omega^*e^{i\Delta t}\hat{\sigma}), \tag{2.84}$$

where $\Delta = \omega - \omega_0$ is the *laser detuning* and the *tilde* notation indicates the operators in the interaction picture. The interaction Hamiltonian $\tilde{V}_{fast}$ oscillates much faster than $\tilde{V}_{slow}$ since $\Delta \ll \omega + \omega_0$ and $\omega_0 \gg 0$ ($\omega_0 \sim 100$THz). To verify the effect of both interactions,

---

[10]   We are assuming $\langle 1|\mathbf{d}|1\rangle = \langle 2|\mathbf{d}|2\rangle = 0$.

[11]   Both Ω and $\tilde{\Omega}$ have the same amplitude $|\Omega| = |\tilde{\Omega}|$ but different phases.

let us calculate the transition amplitude $a_{1\to2}(t)$ from state $|1\rangle$ to state $|2\rangle$ through *time-dependent perturbation theory*,

$$a_{1\to2}(t) = \frac{1}{i\hbar} \int_0^t \langle 2|\tilde{V}(t')|1\rangle \, dt' = \tag{2.85}$$

$$= \frac{1}{i\hbar} \left[\int_0^t \langle 2|\tilde{V}_{fast}(t')|1\rangle \, dt' + \int_0^t \langle 2|\tilde{V}_{slow}(t')|1\rangle \, dt' \right] = \tag{2.86}$$

$$= \frac{\tilde{\Omega}}{2(\omega + \omega_0)}(e^{i(\omega - \omega_0)t} - 1) + \frac{\Omega}{2\Delta}(e^{-i\Delta t} - 1). \tag{2.87}$$

We can neglect the terms with $\tilde{\Omega}$ since $\Delta \ll \omega + \omega_0$ in equation (2.87). In other words, we can neglect the $\tilde{V}_{fast}$ such that $\tilde{V} \simeq \tilde{V}_{slow}$, which is called **rotating-wave approximation**.

2.3.2 Optical Bloch equations

Let us consider the unitary transformation $\hat{U}_{rot} = \hat{\sigma}\hat{\sigma}^\dagger + \hat{\sigma}^\dagger\hat{\sigma}e^{-i\Delta t}$ into the *rotating frame* aiming to eliminate the time-dependence in equation the interaction Hamiltonian (**??**) in the rotating wave approximation so that

$$\tilde{V}' = \hat{U}_{rot}^\dagger \tilde{V} \hat{U}_{rot} + i\hbar(\partial_t \hat{U}_{rot}^\dagger)\hat{U}_{rot} = \frac{\hbar}{2}\begin{bmatrix} 0 & \Omega^* \\ \Omega & -2\Delta \end{bmatrix}. \tag{2.88}$$

Then, applying the unitary transformations to the interaction picture and rotating frame in the density operator $\hat{\rho}$ as well, we obtain the density operator $\tilde{\rho}'$ given by

$$\tilde{\rho}' = \begin{bmatrix} (1+p)/2 & q^*e^{-i\omega t} \\ qe^{i\omega t} & (1-p)/2 \end{bmatrix}. \tag{2.89}$$

From equations (2.59) and (2.89), we can see that $\hat{\rho}$ and $\tilde{\rho}'$ are pretty similar. The only difference are the coherences, which gain an additional phase factor $e^{i\omega t}$ after the transformations. Then, by simplicity, we shall assume $q' = qe^{i\omega t}$.

The master equation (2.72) for our system is given by

$$\partial_t \tilde{\rho}' = -\frac{i}{\hbar}[\tilde{V}', \tilde{\rho}'] + \frac{\Gamma}{2}(2\hat{\sigma}\tilde{\rho}'\hat{\sigma}^\dagger - \{\hat{\sigma}^\dagger\hat{\sigma}, \tilde{\rho}'\}), \tag{2.90}$$

where Γ is a decay rate associated with spontaneous emission. By simplicity, let us assume Ω a positive real value, since any phase of Ω can be incorporate in the coherence q. From now on, we shall consider $q' \to q$ and $\rho'_{1,2} \to \rho_{1,2}$ to simplify the notation, keeping in mind that p and q are evaluated on the rotating frame and in the interaction picture. Thus, evaluating the matrix elements of $\partial_t \tilde{\rho}'$, we obtain

$$\partial_t \rho_{1,1} = -\Omega \, \text{Im}[\rho_{1,2}] + \Gamma \rho_{2,2} \tag{2.91}$$

$$\partial_t \rho_{2,2} = \Omega \, \text{Im}[\rho_{1,2}] - \Gamma \rho_{2,2} \tag{2.92}$$

$$\partial_t \rho_{1,2} = -(\Gamma/2 - i\Delta)\rho_{1,2} + i\Omega(\rho_{1,1} - \rho_{2,2})/2 \tag{2.93}$$

$$\partial_t \rho_{2,1} = -(\Gamma/2 + i\Delta)\rho_{2,1} - i\Omega(\rho_{1,1} - \rho_{2,2})/2, \tag{2.94}$$

where $\rho_{2,1} = (\rho_{1,2})^*$ and $\rho_{1,1} + \rho_{2,2} = 1$. The equations (2.91), (2.92), (2.93), and (2.94) are known as **optical Bloch equations** (OBEs). We can represent these equations in a convenient form through the *Bloch vector* $\mathbf{a}(t)$ given by equation (2.58), so that

$$\partial_t \mathbf{a}(t) = \mathcal{M}\mathbf{a}(t) + \mathbf{b}, \tag{2.95}$$

$$\mathcal{M} = \begin{bmatrix} -\Gamma/2 & -\Delta & 0 \\ \Delta & -\Gamma/2 & -\Omega \\ 0 & \Omega & -\Gamma \end{bmatrix}, \quad \mathbf{b} = \begin{bmatrix} 0 \\ 0 \\ \Gamma \end{bmatrix}, \quad \mathbf{a}(t) = \begin{bmatrix} 2\operatorname{Re}[q(t)] \\ 2\operatorname{Im}[q(t)] \\ p(t) \end{bmatrix}. \tag{2.96}$$

It is labour to solve the equation (2.95) for a general case. *H. C. Torrey* (32) deduced a general form using the *Laplace transformation* but he only obtain exact solutions for the cases of exact resonance $\Delta = 0$ and strong excitation so that $\Omega \gg \Gamma$. We shall pursue the solution of the OBEs from a different approach based upon the calculation of *eigenvalues* and *eigenvectors*.

2.3.2.1 General solution

Considering the vector $\vec{\xi}(t) = \mathbf{a}(t) + \mathcal{M}^{-1}$, where $\mathcal{M}^{-1}$ is the inverse[12] of $\mathbf{M}$, we can rewrite the equation (2.95) so that

$$\partial_t \vec{\xi}(t) = \mathcal{M}\vec{\xi}. \tag{2.97}$$

The equation (2.97) is similar to the Schrodinger equation, $\hat{H}|\psi\rangle = i\hbar\partial_t|\psi\rangle$. Then, since $\mathcal{M}$ is time-independent, we can consider a time evolution given by

$$\vec{\xi}(t) = \sum_{i=1}^{3} c_i e^{m_i t} \vec{\chi}_i = \begin{bmatrix} \xi_1 \\ \xi_2 \\ \xi_3 \end{bmatrix} = \begin{bmatrix} 2\operatorname{Re}[q_\xi(t)] \\ 2\operatorname{Im}[q_\xi(t)] \\ p_\xi \end{bmatrix}, \tag{2.98}$$

where m_1, m_2, and m_3 are *eigenvalues*[13], $\vec{\chi}_1$, $\vec{\chi}_2$. and $\vec{\chi}_3$ are *eigenvectors*, and c_1, c_2, and c_3 are constants ($\partial_t c_i = 0$) which depend on the initial conditions. The eigenvalues are roots of the *characteristic polynomial* given by

$$P(m) = -\det(\mathcal{M} - m\mathbb{I}) \tag{2.99}$$

$$= (\Gamma/2 + m)^2(\Gamma + m) + \Omega^2(\Gamma/2 + m) + \Delta^2(\Gamma + m). \tag{2.100}$$

Since $P(m)$ is a *cubic polynomial* with real coefficients, at least one root is real and the other two are complex conjugate of each other. By the *Routh-Hurwitz criterion*[14], all real parts of the roots are negative numbers. Therefore, the eigenvalues can be written as

$$m_1 = -a, \quad m_2 = -b + ic, \quad \text{and} \quad m_3 = -b - ic, \tag{2.101}$$

[12] We are assuming $\det\mathcal{M} \neq 0$, which is a requirement to exist the inverse of $\mathcal{M}$.
[13] Since $\mathcal{M}$ is not hermitian, its eigenvalues can be complex numbers.
[14] Given a cubic polynomial $f(x) = c_0 + c_1 x + c_2 x^2 + x^3$, if c_0, c_1, and c_2 are positive and $c_2 c_1 > c_0$, then all roots have negative real parts.

where a, b, and c are real values, being a and b positive numbers. Thus, plugging (2.101) in (2.97), we obtain the general solution given by

$$a_i(t) = A_i e^{-at} + e^{-bt}[B_i \cos(ct) + C_i \sin(ct)] + a_i(\infty), \quad \text{for } i \in \{1, 2, 3\}, \qquad (2.102)$$

where a_1, a_2, and a_3 are components of the Bloch vector $\mathbf{a}$ and A_i, B_i, and C_i are complex constants that depend on the initial conditions and the eigenvectors $\vec{\chi}_i$. The first term of (2.102) represents exponential decays of the populations and coherences, which come from the relaxation due to the spontaneous emission. The second and third terms are associated with damped oscillations known as **Rabi oscillations** or **Rabi flopping** (sections 2.3.4 and 2.3.5). The last term is a **stationary** solution (section 2.3.3) in which any oscillation vanishes.

2.3.3 Steady state

After a while, the system will reach a **steady-state** $\mathbf{a}(\infty)$ as shown in equation (2.102). This solution comes straightforwardly from equation (2.95) assuming $\partial_t \mathbf{a}(\infty) = 0$ such that

$$\mathcal{M}\mathbf{a}(\infty) + \mathbf{b} = 0 \Rightarrow \mathbf{a}(\infty) = -\mathcal{M}^{-1}\mathbf{b}, \qquad (2.103)$$

where $\mathcal{M}^{-1}$ is the inverse of $\mathcal{M}$ given by

$$\mathcal{M}^{-1} = \frac{\text{adj}\mathcal{M}}{\det \mathcal{M}}, \quad \det \mathcal{M} = -\Gamma(\Gamma^2/4 + \Omega^2/2 + \Delta^2) \qquad (2.104)$$

$$\text{adj}\mathcal{M} = \begin{bmatrix} \Gamma^2/2 + \Omega^2 & -\Delta\Gamma & \Delta\Omega \\ \Delta\Gamma & \Gamma^2/2 & -\Omega\Gamma/2 \\ \Delta\Omega & \Omega\Gamma/2 & \Gamma^2/4 + \Delta^2 \end{bmatrix}, \qquad (2.105)$$

where $\text{adj}\mathcal{M}$ and $\det \mathcal{M}$ are the *adjugate*[15] and the *determinant* of $\mathcal{M}$ respectively. Thus, the **stationary solution** is given by

$$\mathbf{a}(\infty) = \frac{1}{\Gamma^2/4 + \Omega^2/2 + \Delta^2} \begin{bmatrix} \Delta\Omega \\ -\Omega\Gamma/2 \\ \Delta^2 + \Gamma^2/4 \end{bmatrix} = \begin{bmatrix} 2\,\text{Re}[q'] \\ 2\,\text{Im}[q'] \\ p \end{bmatrix} = \begin{bmatrix} 2\,\text{Re}[qe^{i\omega t}] \\ 2\,\text{Im}[qe^{i\omega t}] \\ p \end{bmatrix}, \qquad (2.106)$$

$$p(\infty) = \frac{\Delta^2 + \Gamma^2/4}{\Delta^2 + \Omega^2/2 + \Gamma^2/4} \quad \text{and} \qquad (2.107)$$

$$q(\infty) = \frac{\Omega}{2} \frac{\Delta - i(\Gamma/2)}{\Delta^2 + \Omega^2/2 + \Gamma^2/4} \qquad (2.108)$$

From equation (2.107), the population of the excited state is given by

$$\rho_{2,2}(\infty) = \frac{1}{2} \frac{\Omega^2/2}{\Delta^2 + \Omega^2/2 + \Gamma^2/4}. \qquad (2.109)$$

For strong excitation such that $\Omega^2 \gg 2\Delta^2 + \Gamma^2/2$, the population inversion saturates $p(\infty) \to 0$ as well as the population of the excited state $\rho_{2,2} \to 1/2$. For weak excitation such that $\Omega^2 \ll 2\Delta^2 + \Gamma^2/2$, $p(\infty) \to 1$ and then $\rho_{2,2} \to 0$.

---

[15]   The adjugate of a matrix is the transpose of its cofactor matrix.

2.3.4 Rabi oscillations

The Rabi oscillations occur during the transient to the steady-state as shown in equation (2.102). They are fully associated with the *coherent evolution* given by the term $[\hat{H}, \hat{\rho}]$ in the master equation (2.90). These oscillations are damped by spontaneous emission, which is an incoherent process. Then, to clearly approach this effect, let us assume a system under strong excitation $\Omega \gg \Gamma$ so that spontaneous emission can be neglected over a considerable period t. In this case, $\vec{\xi}(t) \simeq \mathbf{a}(t)$ in equation (2.98) since $\mathcal{M}^{-1}\mathbf{b} \simeq 0$. The characteristic polynomial (2.100) and its roots are given by

$$P(m) = m(m^2 + |\Omega|^2 + \Delta^2) \quad \Rightarrow \quad m_1 = 0, \quad m_2 = -iG, \quad m_3 = iG, \tag{2.110}$$

where $G \equiv \sqrt{|\Omega|^2 + \Delta^2}$ is the **generalized Rabi frequency**. Plugging the values (2.110) in $\mathcal{M}\vec{\chi}_i = m_i\vec{\chi}_i$, we obtain the following eigenvectors

$$\vec{\chi}_1 = \begin{bmatrix} 1 \\ 0 \\ \Delta/\Omega \end{bmatrix}, \quad \vec{\chi}_2 = \begin{bmatrix} \Delta/\Omega \\ i(G/\Omega) \\ -1 \end{bmatrix}, \quad \vec{\chi}_3 = \begin{bmatrix} -\Delta/\Omega \\ i(G/\Omega) \\ 1 \end{bmatrix}. \tag{2.111}$$

Let us assume an atom initially in the ground state so that $p(0) = 1$ and $q(0) = 0$. Then, from equations (2.98) and (2.111), we obtain

$$\mathbf{a}(0) = \begin{bmatrix} 0 \\ 0 \\ 1 \end{bmatrix} = c_1 \begin{bmatrix} 1 \\ 0 \\ \Delta/\Omega \end{bmatrix} + c_2 \begin{bmatrix} \Delta/\Omega \\ i(G/\Omega) \\ -1 \end{bmatrix} + c_3 \begin{bmatrix} -\Delta/\Omega \\ i(G/\Omega) \\ 1 \end{bmatrix}. \tag{2.112}$$

Solving the system (2.112) of linear equations, we obtain

$$c_1 = \frac{\Delta\Omega}{G^2} \quad \text{and} \quad c_2 = -c_3 = -\frac{\Omega^2}{2G^2}. \tag{2.113}$$

Plugging the values (2.110), (2.111) and (2.113) in (2.98), we obtain

$$p(t) = \frac{\Omega^2}{G^2}\left[\frac{\Delta^2}{\Omega^2} + \cos(Gt)\right] \quad \text{and} \tag{2.114}$$

$$q(t) = \frac{\Omega}{2G^2}[\Delta(1 - \cos(Gt)) - iG\sin(Gt)]. \tag{2.115}$$

Finally, from equation (2.114), the population of the excited state is given by

$$\rho_{2,2}(t) = \frac{1 + p(t)}{2} = \frac{\Omega^2}{2G^2}[1 - \cos(Gt)]. \tag{2.116}$$
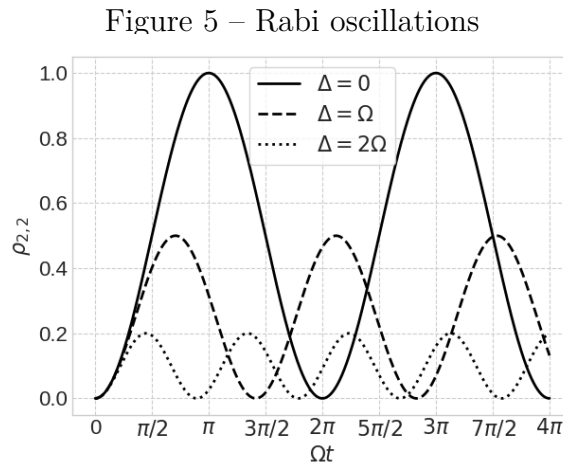
In the exact resonance $\Delta = 0$,

$$p(t) = \cos(\Omega t) \tag{2.117}$$

$$q(t) = i\sin(\Omega t). \tag{2.118}$$

Equation (2.116) reveals oscillations between the ground and excited states at frequency G and period $T = 2\pi/G$. This phenomenon is called **Rabi oscillations** or **Rabi flopping**. Roughly, the ups and downs can be seen as absorptions and stimulated emissions respectively. Furthermore, the amplitude of the oscillations is given

$$\frac{\Omega^2}{G^2} = \frac{\Omega^2}{\Omega^2 + \Delta^2} = \frac{1}{1 + (\Delta/\Omega)^2}, \tag{2.119}$$

which has the maximum 1 when $\Delta = 0$, decreasing with Δ/Ω. Figure 5 illustrates the Rabi oscillations for a few detunings.

Figure 5 – Rabi oscillations

Population of the excited state for Rabi oscillations with detunings equal to 0 (exact resonance), Ω, and 2Ω.
Source: Author

In the exact resonance given by the equations (2.117) and (2.118), the period is $T = 2\pi/\Omega$. If a field is turned on at $t = 0$ and then turned off after $t = T/2$, an atom initially in the ground state will be certainly promoted to the excited state. Such pulse is called π**-pulse**. Furthermore, if a filed is turned on for a duration $T/4$, an atom initially in the ground state ends up in a superposition between the excited and ground states, which is called $\pi/2$**-pulse**. This is widely used in atomic clocks and quantum computation, beyond the scope of this thesis.

2.3.5 Damped Rabi oscillations

When spontaneous emission is consirable, the Rabi oscillations will be damped by them so that, after a while, the system will reach the steady-state given by (2.107) and (2.108). To get some insight into the damping oscillations, let us analyze the case of exact resonance $\Delta = 0$, which has a friendly exact solution. Afterwards, we perform numerical calculations to evaluate the dependence of the damping coefficients a and b, and the oscillation frequency c in (2.102) with the parameters Ω, Δ, and Γ.

2.3.5.1 Exact resonance

In the exact resonance case $\Delta = 0$, the roots of the characteristic polynomial (2.100) have a friendly form given by

$$m_1 = -\frac{\Gamma}{2}, \quad m_2 = -\left(\frac{3\Gamma}{4} + i\Omega_\Gamma\right), \quad m_3 = -\left(\frac{3\Gamma}{4} - i\Omega_\Gamma\right), \tag{2.120}$$

where $\Omega_\Gamma \equiv \sqrt{\Omega^2 - (\Gamma/4)^2}$ is the Rabi oscillations frequency in the presence of damping. Plugging these eigenvalues in $\mathcal{M}\vec{\chi}_i = m_i\vec{\chi}$, we obtain the following eigenvectors

$$\vec{\chi}_1 = \begin{bmatrix} 1 \\ 0 \\ 0 \end{bmatrix}, \quad \vec{\chi}_2 = \begin{bmatrix} 0 \\ 1 \\ e^{i\theta} \end{bmatrix}, \quad \vec{\chi}_3 = \begin{bmatrix} 0 \\ 1 \\ e^{-i\theta} \end{bmatrix}, \tag{2.121}$$

where $\tan\theta = 4\Omega_\Gamma/\Gamma$. Again, let us consider an atom initially in the ground state so that

$$\vec{\xi}(0) = \mathbf{a}(0) - \mathbf{a}(\infty) = \begin{bmatrix} 0 \\ 0 \\ 1 \end{bmatrix} - \begin{bmatrix} 2\operatorname{Re}[q(\infty)] \\ 2\operatorname{Im}[q(\infty)] \\ p(\infty) \end{bmatrix} = (1 - p(\infty))\begin{bmatrix} 0 \\ \Gamma/\Omega \\ 1 \end{bmatrix}. \tag{2.122}$$

Thus, plugging the values (2.120) and (2.121) in (2.98) and assuming the initial conditions (2.122), we obtain

$$c_1\begin{bmatrix} 1 \\ 0 \\ 0 \end{bmatrix} + c_2\begin{bmatrix} 0 \\ 1 \\ e^{i\theta} \end{bmatrix} + c_3\begin{bmatrix} 0 \\ 1 \\ e^{-i\theta} \end{bmatrix} = (1 - p(\infty))\begin{bmatrix} 0 \\ \Gamma/\Omega \\ 1 \end{bmatrix}, \tag{2.123}$$

which is a system of linear equations. After some algebra, the solution of (2.123) is

$$c_1 = 0, \quad c_2 = c_3^* = \left[\frac{\Gamma}{2\Omega} - i\frac{\Omega^2 - \Gamma^2/4}{2\Omega\Omega_\Gamma}\right](1 - p(\infty)). \tag{2.124}$$

Then, we plug (2.124), (2.120), and (2.121) in (2.98), obtaining

$$p_\xi(t) = e^{-3\Gamma t/4}(1 - p(\infty))\left[\cos(\Omega_\Gamma t) + \frac{3\Gamma}{4\Omega_\Gamma}\sin(\Omega_\Gamma t)\right] \quad \text{and} \tag{2.125}$$

$$q_\xi(t) = ie^{-3\Gamma t/4}(1 - p(\infty))\frac{\Gamma}{2\Omega}\left[\cos(\Omega_\Gamma t) - \frac{\Omega^2 - \Gamma^2/4}{\Gamma\Omega_\Gamma}\sin(\Omega_\Gamma t)\right]. \tag{2.126}$$

Finally, plugging the equations (2.125) and (2.126) in $\mathbf{a}(t) = \vec{\xi}(t) + \mathbf{a}(\infty)$, we obtain

$$p(t) = e^{-3\Gamma t/4}(1 - p(\infty))\left[\cos(\Omega_\Gamma t) + \frac{3\Gamma}{4\Omega_\Gamma}\sin(\Omega_\Gamma t)\right] + p(\infty) \quad \text{and} \tag{2.127}$$

$$q(t) = i(1 - p(\infty))\frac{\Gamma}{2\Omega}\left\{e^{-3\Gamma t/4}\left[\cos(\Omega_\Gamma t) - \frac{\Omega^2 - \Gamma^2/4}{\Gamma\Omega_\Gamma}\sin(\Omega_\Gamma t)\right] - 1\right\}. \tag{2.128}$$

The equation (2.127) shows a *damped oscillation* illustrated in figure 6. The damping effect is as strong as the spontaneous emission so that the oscillation vanishes at a decay rate $3\Gamma/4$. Furthermore, when Γ approaches 4Ω, the oscillations also vanish since Ω_Γ tends to zero.

Figure 6 – Damped Rabi oscillations
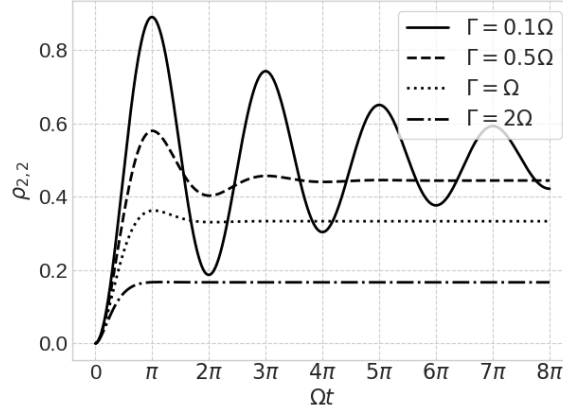
Source: Author

Population of the excited state for damped Rabi oscillations with relaxation rates equal to 0 (exact resonance), $\Omega/2$, Ω, and 2Ω.

2.3.5.2 Numerical solution

There is not a simple analytical solution for the general case (2.102) since the roots of the characteristic polynomial (2.100) do not have a friendly form out of specific regimes such as strong excitation (section 2.3.4) and exact resonance (2.3.5.1). Then, to evaluate the coefficients a and b, and the oscillation frequency c, we numerically calculate the eigenvalues of $\mathcal{M}$. These eigenvalues are associated with the coefficients a, b, and c through (2.101).

Figure 7 – Damping coefficients a and b
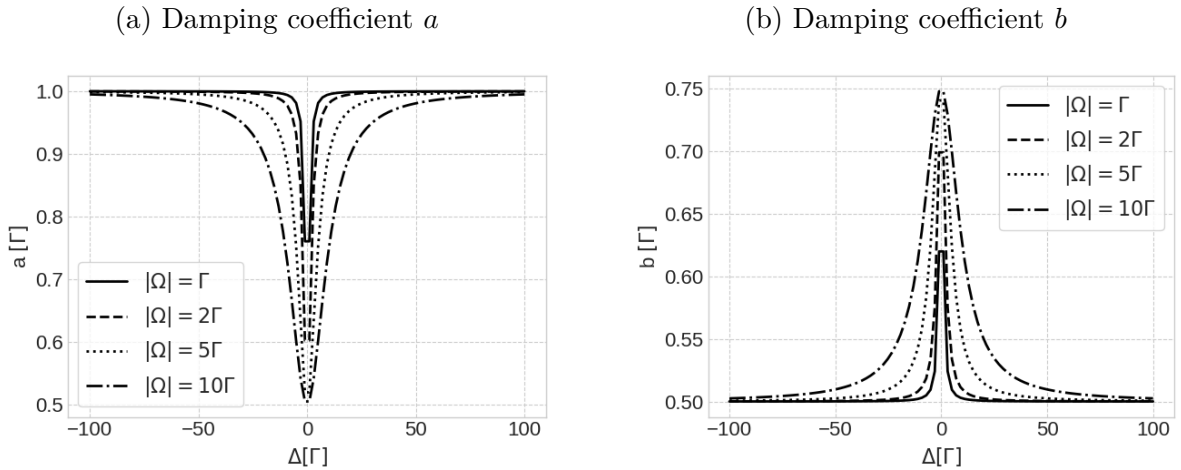
(a) Damping coefficient a (b) Damping coefficient b

Damping coefficient a from equation (2.102) in function of the detuning Δ for different Rabi frequencies Ω.

Damping coefficient b from equation (2.102) in function of the detuning Δ for different Rabi frequencies Ω.

Source: Author

The damping coefficient a from equation (2.102) is the rate at which the populations and coherences decay. From figure 7a, we can see that a converges to Γ when $a \to \pm\infty$. Also, the coefficient a is between $\Gamma/2$ and Γ. The damping coefficient b from

equation (2.102) is a rate at which the Rabi oscillations decay. From figure 7b, we can see that b converges to $\Gamma/2$ when $b \to \pm\infty$ and it is between $\Gamma/2$ and $3\Gamma/4$. The lower the Rabi frequency the faster a and b converge. The system practically reaches the steady-state for a time greater than $2/\Gamma$, since both damping coefficients have the minimum $\Gamma/2$.

Figure 8 – Oscillation frequency c
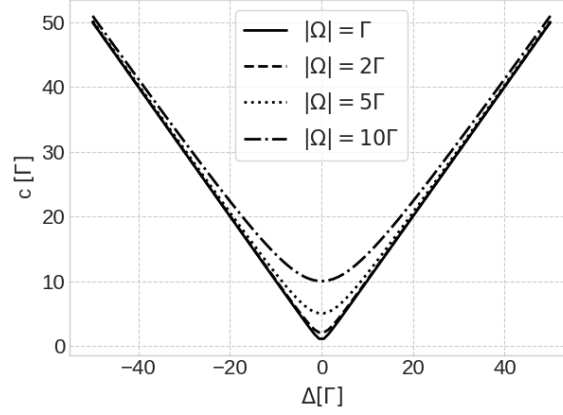
Source: Author
Oscillation frequency c from equation (2.102) in function of the detuning Δ for different Rabi frequencies Ω.

The coefficient c from equation (2.102) is the frequency at which the system oscillates (Rabi oscillations). From figure 8, we can see that c increases linearly for higher detunings so that $c = |\Delta|$. For lower detunings, c converges to $\Omega_\Gamma = \sqrt{\Omega^2 - (\Gamma/4)^2}$.

2.3.6 Rate-equation limit

The OBEs become the Einstein rate equations when the coherent effects do not play a role. Then, we can derived the Einstein equations eliminating the coherence q in the OBEs adiabatically. Let us assume a slow population dynamics so that the coherence decay much faster than the populations. Thus, $\partial_t q \simeq 0$ in the time scale of the population dynamics. This is called **adiabatic approximation** and it is valid when there is a considerable collision rate[16] γ so that $\gamma \gg \Gamma, \Omega$. In this regime, from equations (2.91), (2.92), (2.93) and (2.94), we obtain

$$\partial_t \rho_{2,2} = (1 - 2\rho_{2,2}) \frac{\Omega}{2} \frac{2\Omega/\Gamma}{1 + (2\Delta/\Gamma)^2} - \Gamma\rho_{2,2}, \tag{2.129}$$

where we assume $\partial_t \rho_{1,2} = \partial_t \rho_{2,1} = 0$ and $\rho_{1,1} = 1 - \rho_{22}$. Comparing equations (2.129) and (2.20), we associate

$$A \to \Gamma \quad \text{and} \quad \alpha(\Delta) = \Omega \frac{2\Omega/\Gamma}{1 + (2\Delta/\Gamma)^2}, \tag{2.130}$$

---

[16]   The collision rate is associated with pure dephasing terms in the Lindblad superoperator (2.73)

where α is the *pumping rate*. Therefore, the *saturation parameter* $s(\Delta) = \alpha(\Delta)/A$ is given by

$$s(\Delta) = \frac{2\Omega^2/\Gamma^2}{1 + (2\Delta/\Gamma)^2} = \frac{s_0}{1 + (2\Delta/\Gamma)^2}, \quad s_0 \equiv s(0) = \frac{2\Omega^2}{\Gamma^2}, \tag{2.131}$$

where s_0 is the **resonant saturation parameter**. Thus, comparing equations (2.22) and (2.131), we obtain

$$s_0 = \frac{I_0}{I_s} = \frac{2\Omega^2}{\Gamma^2} \quad \text{and} \quad g(\Delta) = \frac{g(0)}{1 + (2\Delta/\Gamma)^2}, \tag{2.132}$$

where $g(\Delta)$ is the *line shape function* and I_s is the *saturation parameter*. Since g must be normalized, we have

$$\int_{-\infty}^{\infty} g(\Delta)d\Delta = 1 \Rightarrow g(0) = \frac{2}{\pi\Gamma} \Rightarrow g(\Delta) = \frac{1}{\pi}\frac{\Gamma/2}{\Delta^2 + (\Gamma/2)^2} = \frac{2}{\pi\Gamma}\frac{1}{1 + (2\Delta/\Gamma)^2}, \tag{2.133}$$

where $g(\Delta)$ is a *Lorentzian function* whose centre is at $\Delta = 0$ and FWHM is Γ. From equations (2.32), (2.33), and (2.131), we obtain

$$\sigma(\Delta) = \frac{\hbar\omega_0}{I_s}\frac{\Gamma}{2}\frac{1}{1 + (2\Delta/\Gamma)^2} = \frac{\sigma_0}{1 + (2\Delta/\Gamma)^2} \quad \text{and} \tag{2.134}$$

$$\sigma_{abs}(\Delta) = \frac{\hbar\omega_0}{I_0}\frac{\Gamma}{2}\frac{s_0}{1 + s_0 + (2\Delta/\Gamma)^2} = \frac{\sigma_0}{1 + s_0 + (2\Delta/\Gamma)^2}. \tag{2.135}$$

Even if $\partial_t q$ is not negligible, i.e. the coherence and populations dynamics are in the same time scale, it is possible to compare the stationary solution of the OBEs and the Einstein equations in thermal equilibrium. In this case, we should obtain the same equations deduced above if we compare (2.21) and (2.109).

It is convenient to rewrite equations (2.107) and (2.108) in terms of the saturation parameter so that

$$p(\infty) = \frac{1}{1 + s(\Delta)} = \frac{1 + (2\Delta/\Gamma)^2}{1 + s_0 + (2\Delta/\Gamma)^2}, \tag{2.136}$$

$$q(\infty) = \rho_{2,1} = \frac{\Gamma}{2\Omega}\frac{s(\Delta)}{1 + s(\Delta)}(2\Delta/\Gamma - i) = \frac{\Gamma}{2\Omega}\frac{s_0}{1 + s_0 + (2\Delta/\Gamma)^2}(2\Delta/\Gamma - i). \tag{2.137}$$

2.3.7 Scattering cross section

In atomic spectroscopy, it is often measure the light power P_{sc} which an atom emits due to spontaneous emission, i.e. the power of the scattered light also known as **fluorescence**. Fluorescence imaging can be used to detect single trapped atoms (33) and momentum distribution (34, 35). In the case of a two-level atom interacting with a monochromatic light whose frequency is ω, we can write P_{sc} as the energy $\hbar\omega_0$[17] of a

---

[17] The spontaneously emitted photon does not have a single frequency ω_0 (section 2.1.3). However, since ω_0 is much greater than the FWHM of the line shape, we have

$$\omega_0 \simeq \int_0^{\infty} \omega g(\omega)d\omega$$

.

single photon with frequency ω_0 (atomic resonant frequency) times the rate $R_{sc} = \Gamma\rho_{2,2}$[18] at which an atom scatters photons, i.e. the rate at which an atom absorb a photon stimulately and then emit it spontaneously. Therefore, we can define a cross section given by[19].

$$\sigma_{sc}(\Delta) = \frac{P_{sc}}{I_0} = \frac{\hbar\omega_0}{I_0}\Gamma\rho_{2,2} = \frac{\hbar\omega_0}{I_0}\frac{\Gamma}{2}\frac{s_0}{1+s_0+(2\Delta/\Gamma)^2}, \tag{2.138}$$

where I_0 is the light intensity. The quantity σ_{sc} is called **scattering cross section** and it is related to the probability of happening a scattering event, i.e, the probability of absorbing a photon and then emitting it spontaneously. From equation (2.134), we have $\sigma_{sc} = \sigma_{abs}$, which is expected due to conservation of energy, i.e. the energy lost from a incident light beam must be convert to scattering light via spontaneous emission. Overall, the total absorption cross section σ_{abs} (section 2.1.5) is associated with *absorption imaging* and the scattering cross section σ_{sc} is associated with *fluorescence imaging*.

2.3.8 Line-broadening mechanisms

In section 2.1.3, we introduce the *line shape function $g(\omega)$*, which gives the probability of either absorbing or emitting a photon with a frequency between ω and $\omega+d\omega$. This function is proportional to the *absorption cross-section $\sigma(\omega)$* according equation (2.32). Although the line shape function take spectral broadening into account, it is not directly proportional to both absorbing and fluorescence profiles, which are actually measured. Theses profiles are associated directly with the *net absorption cross-section σ_{abs}* and the *scattering cross-section σ_{sc}*. From equations (2.135) and (2.138), we can see that the absorption profile is not a sharp line as discussed in section 2.1.3. In the next sections, we shall discuss physical effects which can both broaden and shift the absorption/scattering cross-section profile. Overall, there are two types of line broadening mechanisms:

- **Homogeneous broadening:** all atoms in a medium are affected in the same way. In this case, we can add these line-broadening mechanisms in the optical Bloch equations so that it is valid for all atoms in the medium;

- **Inhomogeneous broadening:** each atom in a medium is individually affected. In this case, we can only described line-broadening mechanisms in the optical Bloch equations for individual atoms. Therefore, we can not generalize for all atoms in the medium.

---

[18] Γ is the rate at which atoms in the excited state emit photons spontaneously and $\rho_{2,2}$ is the probability of finding an atom in the excited state.

[19] In a general case,

$$P_{sc} = \int \sigma_{sc}(\omega')I(\omega')d\omega',$$

where $I(\omega')$ is the spectral intensity. However, since $I(\omega') = I_0\delta(\omega'-\omega)$ for a monochromatic light, we can write $P_{sc} = \sigma_{sc}(\omega)I_0$.

2.3.8.1 Natural broadening

Let us assume an isolated atom initially in the excited state so that there is not an incident light beam ($s_0 = 0$). This atom will decay in an average time $1/\Gamma$ known as *lifetime*. In other words, $1/\Gamma$ is the average time for the system changes considerably. Therefore, due to the *time-energy uncertainty principle*, there will be an energy uncertainty in the excited state given by

$$\Delta E \geq \frac{\hbar}{2\Delta t} = \frac{\hbar\Gamma}{2}. \tag{2.139}$$

Spontaneously emitted photons do not have a deterministic energy $\hbar\omega_0$ since the system

Figure 9 – Natural broadening
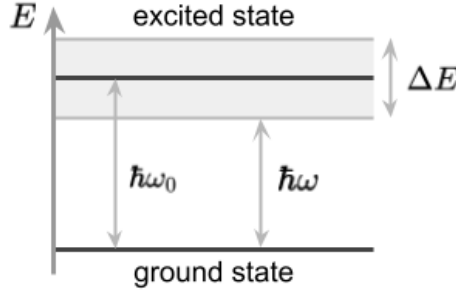
Energy uncertainty of a excited state whose lifetime is $1/\Gamma$. Due to the time-energy uncertainty principle, $\Delta E \geq \hbar\Gamma/2$ and then a spontaneously emitted photon have a random energy $\hbar\omega$ whose the average is $\hbar\omega_0$ and the uncertainty is greater than $\hbar\Gamma/2$.
Source: Author

does not have either, as illustrated in figure 9. This phenomena provokes a *homogeneous* line-broadening known as **natural broadening** or **lifetime broadening**. The probability of spontaneously emitting a photon with frequency between ω and $\omega + d\omega$ is given by the line shape function $g(\omega)$ and it is proportional to the absorption cross-section $\sigma(\omega)$ according equations (2.133) and (2.134). From equation (2.133), we have

$$g(\Delta) = \frac{1}{\pi}\frac{\Gamma/2}{\Delta^2 + (\Gamma/2)^2}. \tag{2.140}$$

The equation (2.140) is *Lorentzian profile* whose FWHM, also known as *linewidth*, is Γ, which is in agreement to equation (2.16) proposed in section 2.1.3. Since Γ is associated with the natural broadening, it is also called **natural linewidth**. In the regime of weak excitation so that $s_0 \ll 1$, the absorption cross-section approximately equals the net absorption cross-section such that $\sigma \simeq \sigma_{abs}$.

2.3.8.2 Power broadening

In the presence of a light field so that $s_0 > 0$, the only spectral broadening is the natural broadening given by (2.140). However, the net absorption cross-section σ_{abs} does

not equal the absorption cross-section σ. According to equation (2.33), there will be a decreasing by a factor of $1 + s(\omega)$, which causes a line-broadening illustrated in figure (10). From equations (2.135) and (2.134), we have

$$\sigma(\Delta) = \frac{\pi\Gamma\sigma_0}{2}g(\Delta) \quad \text{and} \quad \sigma_{abs}(\Delta) = \frac{\pi\Gamma\sigma_0}{2(1+s_0)}L(\Delta), \tag{2.141}$$

$$\text{where} \quad L(\Delta) \equiv \frac{2}{\pi\Gamma'}\frac{1}{1+(2\Delta/\Gamma')^2} \quad \text{and} \quad \Gamma' \equiv \Gamma\sqrt{1+s_0}. \tag{2.142}$$

The function L is known as **absorption line-shape** and it is a *Lorentzian profile* whose *FWHM* is Γ'. The quantity Γ' is known as **power-broadened linewidth**. In the regime of weak excitation so that $s_0 \ll 1$, the absorption line-shape becomes the line shape function, $L(\Delta) \to g(\Delta)$, and the power-broadened linewidth becomes the natural linewidth, $\Gamma' \to \Gamma$.

Figure 10 – Net absorption cross-section
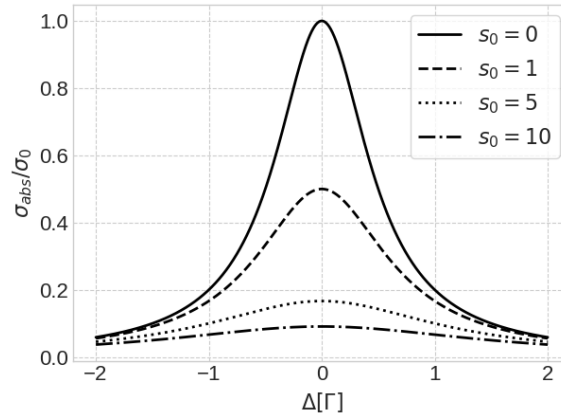
Net absorption cross section as function of detuning for some values of resonant saturation parameter.
Source: Author

2.3.8.3 Doppler broadening

The angular frequency ω' of an incident light beam depends on the frame in which it is being observed. This effect is known as **Doppler effect**. We have been studying the atom-light interaction assuming that the light frequency is the same in both laboratory and atom frames. However, the Doppler effect causes an *inhomogeneous resonance shift* since each atom will perceive an angular frequency given by

$$\omega' = \omega - \mathbf{k} \cdot \mathbf{v}, \tag{2.143}$$

where ω and $\mathbf{k}$ are, respectively, the angular frequency and the wave vector of the light beam in the laboratory frame, and $\mathbf{v}$ is the velocity of the atom also in the laboratory frame. Subtracting the resonant angular frequency ω_0 in both sides of equation (2.143), we obtain

$$\Delta_{eff} = \Delta - \mathbf{k} \cdot \mathbf{v}, \tag{2.144}$$

where $\Delta_{eff} = \omega' - \omega_0$ is the *effective detuning*. We must called $-\mathbf{k} \cdot \mathbf{v}$ as **Doppler shift**. Let us consider a gas following the *Maxwell-Boltzmann distribution* so that the probability $P(v)dv$ of finding an atom with a velocity component between v and $v + dv$ parallel to $\mathbf{k}$ direction is given by

$$P(v)dv = \frac{1}{\alpha\sqrt{2\pi}} \exp\left(-\frac{v^2}{2\alpha^2}\right) dv, \quad \alpha \equiv \sqrt{\frac{k_B T}{m}}, \tag{2.145}$$

where T is the temperature of the gas, k_B is the Boltzmann constant, and m is the atom mass. The equation (2.145) is a **Gaussian distribution** centered at zero whose *standard deviation* is α. Also, the FWHM is approximately 2.355α. If we consider a resonant laser so that $\Delta = 0$ or $\omega = \omega_0$, we can associated an effective absorption line shape given by

$$D(\omega') = \frac{1}{\beta\sqrt{2\pi}} \exp\left[-\frac{(\omega' - \omega_0)^2}{2\beta^2}\right], \quad \beta \equiv \frac{\omega_0}{c}\alpha = \frac{\omega_0}{c}\sqrt{\frac{k_b T}{m}}. \tag{2.146}$$

2.3.9 Optical forces

We can divide the atom state into two sets. The first one is the *internal states* related to the *electronic states*. The second one is the *external states* associated with the centre-of-mass coordinates. So far we evaluated the dynamics of the internal states, neglecting the dynamics of the atomic centre-of-mass except to explain Doppler broadening in section (2.3.8.3). However, there is a coupling between the external and internal degrees of freedom mediated by the absorption and emission processes, which provokes mechanical effects in the atomic centre-of-mass. These effects can be quantify from the *Ehrenfest theorem*, which establishes the average force given by

$$\mathbf{F} = -\langle \nabla \hat{V} \rangle, \tag{2.147}$$

where $\hat{V}$ is the interaction Hamiltonian.

In section 2.3.1, we introduce the interaction Hamiltonian (2.88) assuming an interaction between a two-level atom and a monochromatic light beam in the *rotating frame* and in the *interaction picture*. In the dynamics of the internal states, we can neglect the spatial dependence of the Rabi frequency Ω due to the rotating wave approximation. However, in the dynamics of the external states this spatial variation must be considered. It is important to notice that E_0 can have a spatial dependence by itself when the light beam is not a plane wave, which is the case of a Gaussian beam[20]. Considering $\Omega(\mathbf{r}) = |\Omega(\mathbf{r})|e^{i\mathbf{k}\cdot\mathbf{r}}$[21], we obtain

$$\hat{V}(\mathbf{r}) = \frac{\hbar}{2} \begin{bmatrix} 0 & |\Omega(\mathbf{r})|e^{-i\mathbf{k}\cdot\mathbf{r}} \\ |\Omega(\mathbf{r})|e^{i\mathbf{k}\cdot\mathbf{r}} & -2\Delta \end{bmatrix} \Rightarrow \tag{2.148}$$

$$\nabla \hat{V} = \frac{\hbar}{2} \begin{bmatrix} 0 & (\nabla|\Omega| - i\mathbf{k}|\Omega|)e^{-i\mathbf{k}\cdot\mathbf{r}} \\ (\nabla|\Omega| + i\mathbf{k}|\Omega|)e^{i\mathbf{k}\cdot\mathbf{r}} & 0 \end{bmatrix}, \tag{2.149}$$

---

[20] The Gaussian beam properly described that light beam produces by a laser.
[21] Any additional phase in Ω can be incorporated in the coherence q

We can evaluate the average force (2.147) considering the property (2.48) so that

$$\mathbf{F} = -\operatorname{Tr}\left[\hat{\rho}\nabla\hat{V}\right], \tag{2.150}$$

where $\hat{\rho}$ is the density operator of the two-level atom. As discussed in section 2.3.3, the system will reach a steady-state due to spontaneous emission, a relaxation process. In section 2.3.5.2, we verify that the system reaches the steady-state exponentially at a minimum rate $\Gamma/2$, where Γ is the natural linewidth. If the dynamics time scale is much greater than $2/\Gamma$, we can assume the system in the steady-state. Then, the density operator $\hat{\rho}$ are defined by equations (2.107) and (2.108) and the average force $\mathbf{F}$ is given by

$$\mathbf{F} = -\hbar\operatorname{Re}[(\nabla|\Omega| + i\mathbf{k}|\Omega|)q^*(\infty)]. \tag{2.151}$$

Plugging $q(\infty)$ of equation (2.137) in (2.151), we obtain

$$\mathbf{F} = -\frac{\hbar\Delta}{\Omega}\frac{s(\Delta)}{1+s(\Delta)}\nabla\Omega + \hbar\mathbf{k}\frac{\Gamma}{2}\frac{s(\Delta)}{1+s(\Delta)}. \tag{2.152}$$

We can simply the equation (2.152) considering

$$\nabla\ln\left[1+s(\Delta)\right] = \frac{2}{\Omega}\frac{s(\Delta)}{1+s(\Delta)}\nabla\Omega. \tag{2.153}$$

Then, plugging (2.153) in (2.152), we obtain $\mathbf{F} = \mathbf{F}_{rp} + \mathbf{F}_{dp}$ where

$$\mathbf{F}_{rp} = \hbar\mathbf{k}\frac{\Gamma}{2}\frac{s(\Delta)}{1+s(\Delta)} = \hbar\mathbf{k}\frac{\Gamma}{2}\frac{s_0}{1+s_0+(2\Delta/\Gamma)^2}, \tag{2.154}$$

$$\mathbf{F}_{dp} = -\nabla U_{dp}, \quad U_{dp} = \frac{\hbar\Delta}{2}\ln\left[1+s(\Delta)\right] = \frac{\hbar\Delta}{2}\ln\left[1+\frac{s_0}{1+(2\Delta/\Gamma)^2}\right], \tag{2.155}$$

The dissipative force $\mathbf{F}_{rp}$ is called **radiation pressure force** and the conservative force $\mathbf{F}_{dp}$ is called **gradient dipole force**.

2.3.9.1 Radiation pressure force

We can rewrite $\mathbf{F}_{rp}$ from equation (2.154) considering the scattering cross-section σ_{sc} from equation (2.138) so that

$$\mathbf{F}_{rp} = \hbar\mathbf{k}\frac{I_0}{\hbar\omega_0}\sigma_{sc}(\Delta) = \hbar\mathbf{k}R_{sc}, \quad R_{sc} = \frac{\Gamma}{2}\frac{s_0}{1+s_0+(2\Delta/\Gamma)^2}, \tag{2.156}$$

where $I_0/(\hbar\omega_0)$ is the flux of photons from the incident beam. The quantity R_{sc}, known as **scattering rate**, is the frequency at which an atom absorbs photons from the incident beam and afterwards scatters them out by spontaneous emission. Hence, from equation (2.156), we can interpret the radiation pressure force as the gained momentum after successive events of absorption followed by spontaneous emission. Since the spontaneous emission is isotropic, only the absorption events contribute for the gained momentum as shown in figure (11).

Figure 11 – Radiation pressure force
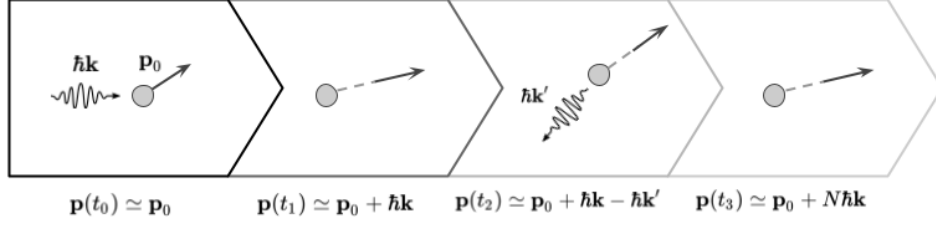
An atom initially with momentum $\mathbf{p}_0$ absorbs a photon with momentum $\hbar\mathbf{k}$ after a period $t_1 - t_0$. Then, at instant t_2, this atom spontaneously emits a photon with momentum $\hbar\mathbf{k}'$ so that $|\mathbf{k}| = |\mathbf{k}'|$. Finally, after successive absorption and emissions, the final momentum will be $\mathbf{p} \simeq \mathbf{p}_0 + N\hbar\mathbf{k}$ since the spontaneous emission is isotropic. The quantity N is the number of absorbed photons after a period $t_3 - t_0$. Therefore, the impulse after a period Δt will be $\Delta\mathbf{p} = \hbar\mathbf{k}R_{sc}\Delta t$, where R_{sc} is the rate at which the atom scatters photons.
Source: Author

From equation (2.156), we can see that the radiation pressure force has the maximum at resonance, and it decreases with the detuning. Also, this force saturates when s_0 is much greater than $1 + (2\Delta/\Gamma)^2$. The spontaneous emission rate determines the force intensity, which is as greater as Γ. Since $\mathbf{F}_{rp}$ is a dissipative force, it can be used to both cool and trap atoms, being a the key concepts to understand MOTs.

2.3.9.2 Gradient dipole force

The gradient dipole force can be derived from a potential U_{dp} illustrated in figure (12), and therefore it is a conservative force. At resonance, U_{dp} is zero and its module increases with the detuning for a range near to resonance. Far from resonance, U_{dp} asymptotically goes into zero. Unlike the radiation pressure force, the gradient dipole force does not saturate. It can increase continuously without bound, though it only does logarithmically for large intensities (saturation parameter). This forces is usually applied to spatially confine atoms.
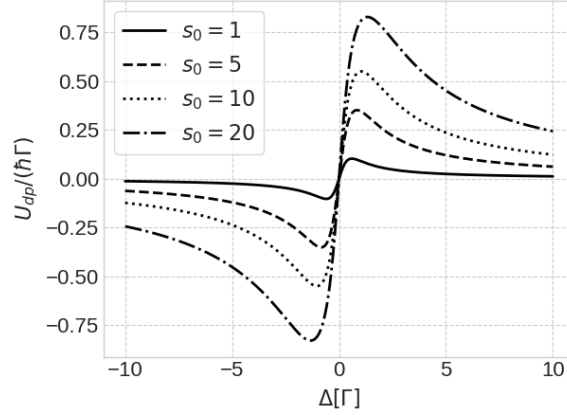
2.3.10 Selection Rules

In section 2.3.1, we verify that electric-dipole transitions depends on the *transition dipole moment* $\vec{\mu}$. When $|\vec{\mu}|$ is greater than zero, the transition is allowed, otherwise the transition is **dipole forbidden**. The transition moment between two arbitrary electronic states $|i\rangle$ and $|j\rangle$ is given by

$$\vec{\mu}_{i,j} = \langle j|\mathbf{d}|i\rangle = -e\,\langle j|\mathbf{r}|i\rangle\,, \tag{2.157}$$

where $\mathbf{r}$ is the electron position. In this section, we shall explore spherical symmetries to obtain conditions in which the transition matrix (2.157) vanishes. These conditions are

Figure 12 – Potential from gradient dipole force

Potential from gradient dipole force for few saturation parameters as a funtion of detuning.
Source: Author

known as **selection rules**. To effectively investigate such symmetries, let us consider the electron position in spherical coordinates so that

$$\mathbf{r} = r \left(\sin\theta \cos\phi \mathbf{e}_x + \sin\theta \sin\phi \mathbf{e}_y + \cos\theta \mathbf{e}_z \right), \tag{2.158}$$

where $\theta \in [0, \pi]$ is the *polar angle*, $\phi \in [0, 2\pi[$ is the *azimuthal angle*, $r \in [0, \infty[$ is the *radial distance*, and $\{\mathbf{e}_x, \mathbf{e}_y, \mathbf{e}_z\}$ is the *Cartesian basis*. It is also convenient to rewrite the position (2.158) on the **spherical basis** given by

$$\left\{ \mathbf{e}_{\pm 1} = \frac{\mp \mathbf{e}_x - i\mathbf{e}_y}{\sqrt{2}} = -(\mathbf{e}_{\mp 1})^*, \ \mathbf{e}_0 = \mathbf{e}_z \right\} \tag{2.159}$$

so that

$$r_\pm = \mp \frac{r}{\sqrt{2}} \sin\theta e^{\mp i\phi} \ \text{ and } \ r_0 = \cos\theta, \ \text{ or} \tag{2.160}$$

$$r_q = \mathbf{r} \cdot \mathbf{e}_q^* = r\sqrt{\frac{4\pi}{3}} Y_{1,-q}(\theta, \phi) \ \text{ for } \ q \in \{-1, 0, 1\}, \tag{2.161}$$

where r_q is a component[22] of $\mathbf{r}$ on the spherical basis and $Y_{l,m}(\theta, \phi)$ is a **spherical harmonic** of degree l and order m.

To evaluate the inner product $\langle i | \mathbf{r} | j \rangle$ in (2.157), we must describe the spatial dependence of $|i\rangle$ and $|j\rangle$. Essentially, an electronic state can be represented by $|n, l, m_l, m_s\rangle$[23] where n, l, m_l and m_s are quantum numbers described below

- *Principal quantum number n*: a positive integer related to the energy and the radial position of the electron;

---

[22] Since the spherical basis is composed of complex elements, we must consider the component of a given $\mathbb{C}^3$-vector $\mathbf{v}$ as $v_\alpha = \mathbf{v} \cdot \mathbf{e}_\alpha^*$.

[23] We are neglecting the hyperfine structure.

- *Orbital angular momentum quantum number l*: a positive number in the range $|l| < n$ associated with the total orbital angular momentum $\mathbf{L}^2$ whose eigenvalues are $\hbar^2 l(l+1)$;

- *Magnetic quantum number m_l*: an integer number in the range $|m_l| \leq l$ related to the z-projection of the orbital angular momentum given by the operator $\hat{L}_z$ whose eigenvalues are $\hbar m_l$;

- *Spin quantum number m_s*: a integer number in the range $|m_s| \leq 1/2$ related to the z-projection of the spin given by the operator $\hat{S}_z$ whose eigenvalues are $\hbar m_s$.

Let us assume $|i\rangle = |n, l, m_l, m_s\rangle$ and $|j\rangle = |n', l', m'_l, m'_s\rangle$ so that $\langle i|r_q|j\rangle = \langle n, l, m_l, m_s|r_q|n', l', m'_l, m'_s\rangle$. Since the spin does not depend on the position, we have $\langle i|r_q|j\rangle = \delta_{m_s, m'_s} \langle n, l, m_l|r_q|n', l', m'_l\rangle$, which means the transition is dipole forbidden when the spin does not remain the same. The angular state $|l, m_l\rangle$ is defined by the *spherical harmonic* $Y_{l,m_l}(\theta, \phi)$ so that, from equation (2.161),

$$\langle n, l, m_l|r_q|n', l', m'_l\rangle \propto \int Y^*_{l,m_l}(\theta, \phi)Y_{1,-q}(\theta, \phi)Y_{l',m'_l}(\theta, \phi)d\Omega \propto \int_0^{2\pi} e^{i(m'_l - m_l - q)\phi}d\phi. \tag{2.162}$$

From the most right term in (2.162), we immediately see that the transition moment is zero when $m'_l - m_l - q \neq 0$, which means the transition is allowed when $\Delta m_l = 0, \pm 1$. The transitions in which $\Delta m_l = 0$ are known as π**-transitions**, whereas the transitions in which $\Delta m_l = \pm 1$ are known as σ**-transitions**.

To evaluate the middle term in (2.162), we shall rewrite the product of two spherical harmonics as a sum of spherical harmonics in the following way[24]

$$Y_{l_1,m_1}Y_{l_2,m_2} = \sum_{j,m_j}(-1)^m \sqrt{\frac{(2l_1+1)(2l_2+1)(2j+1)}{4\pi}} \begin{pmatrix} l_1 & l_2 & j \\ m_1 & m_2 & m_j \end{pmatrix} \begin{pmatrix} l_1 & l_2 & j \\ 0 & 0 & 0 \end{pmatrix} Y_{j,-m_j}, \tag{2.163}$$

where the matrix elements are the **Wigner 3-j symbols** which are directly associated with the **Clebsch-Gordan coefficients**. Thus, plugging $l_1 = 1$, $m_1 = -q$, $l_2 = l'$, and $m_2 = m'_l$ in equation (2.163), we obtain

$$Y_{1,-q}Y_{l',m'_l} = \sum_{j,m_j}(-1)^m \sqrt{\frac{3(2l'+1)(2j+1)}{4\pi}} \begin{pmatrix} 1 & l' & j \\ -q & m'_l & m_j \end{pmatrix} \begin{pmatrix} 1 & l' & j \\ 0 & 0 & 0 \end{pmatrix} Y_{j,-m_j}. \tag{2.164}$$

Then, plugging (2.164) in the middle term of (2.162), we obtain

$$\int Y^*_{l,m_l}(\theta, \phi)Y_{1,-q}(\theta, \phi)Y_{l',m'_l}(\theta, \phi)d\Omega = \sum_{j,m_j} A_{j,m_j} \int Y^*_{l,m_l}(\theta, \phi)Y_{j,-m_j}(\theta, \phi)d\Omega, \tag{2.165}$$

where A_{j,m_j} are constants. Since j satisfies the *triangular condition* $|l'-1| \leq j \leq l'+1$, the right term in (2.165) is only non-zero when $l = l' \pm 1$ due to the orthogonality property.

---

[24] See section 7.3.2 Spherical Harmonics in reference (26).

The case $l = l'$ also seen possible, but the left term in (2.165) is zero due to the parity of the spherical harmonics given by $Y_{l,m}(\mathbf{r}) = (-1)^l Y_{l,m}(\mathbf{r})$, which requires that $l + l' + 1$ to be an even number.

Overall, the selection rules for electric-dipole-transition are given by $\Delta l = \pm 1$, $\Delta m_l = 0, \pm 1$, and $\Delta m_s = 0$. We can see theses rules from another perspective when we consider that an atom absorbs or emits a photon. The total angular momentum of any photon is $2\hbar^2$ ($J = 1$). Therefore, $\Delta l = \pm 1$ and $\Delta m = 0, \pm 1$ follow from the conservation of angular momentum.

Besides the transition matrix, the transition also depends on the polarization vector $\vec{\epsilon}$ of the radiation through the Rabi frequency $\Omega \propto \vec{\mu} \cdot \vec{\epsilon}$ in equation (2.81). Let us consider the polarization in the spherical basis such that

$$\vec{\epsilon} = \sum_{n=-1}^{1} A_n \mathbf{e}_n \quad \text{and} \quad \sum_{n=-1}^{1} |A_n|^2 = 1, \tag{2.166}$$

where A_n is a component of the polarization vector. The components A_{+1} and A_{-1} are related to the right-handed and left-handed circular polarizations respectively, whereas the component A_0 is related to the linear polarization on the z-direction. In the case of π-transitions, the only non-zero component of the electron position is r_0 due to the most right term in equation (2.162). Therefore, these transitions are only induced by linearly polarized light on z-direction. The σ-transitions obey the same logic: right-hand circularly light induces σ^+-transitions ($\Delta m_l = +1$) and left-hand circularly light induces σ^--transitions ($\Delta m_l = -1$).

3 Magneto-Optical Trap

The magneto-optical trap (MOT) is a technique widely used in laser cooling experiments which allows both trapping and cooling of an atomic dilute gas. In this section, we shall approach the MOT theory (12, 36) considering the simplest transition $J = 0 \rightarrow J = 1$, where J is the total angular momentum of the electronic state. To get an insight into the cooling and trapping mechanisms, we first discuss a simplified one-dimensional MOT (1D-MOT) assuming two counter-propagating laser beams and a linear magnetic field[1]. Afterwards, we analyze the three-dimensional case assuming a standard arrangement with six counter-propagating laser beams. Finally, we introduce **narrow-line magneto-optical traps** (nMOTs) (37) by assuming an atomic transition with a natural linewidth (section 2.3.8.1) close to the photonic recoil.

3.1 One-dimensional model

As a first approach to the MOT theory, let us consider a simplified one-dimensional model (1D-MOT) illustrated in figure 13. In this model, two counter-propagating laser beams of opposite circular polarization interact with an atom in the presence of a linear magnetic field $\mathbf{B} = B_0 z \mathbf{e}_z$, where $B_0 > 0$ is the gradient magnitude. Both laser beams have the same angular frequency ω and are tuned close to the transition $J = 0 \rightarrow J = 1$ whose angular frequency is ω_0.

Figure 13 – 1D-MOT
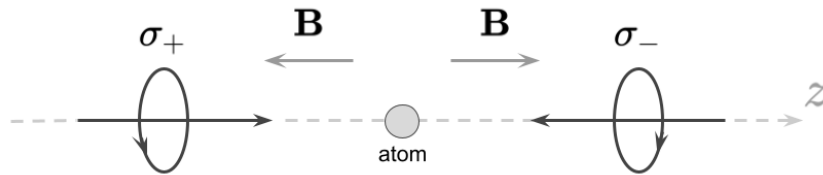
Simplified one-dimensional MOT composed of two counter-propagating laser beams and a linear magnetic field $\mathbf{B} = B_0 z \mathbf{e}_z$, where $B_0 > 0$. We consider the σ_+ and σ_- beams right-handed and left-handed polarized respectively.
Source: Author

Disregarding the magnetic field, the transition is properly represented by a degenerate *two-level system* whose energy difference is $\hbar\omega_0$. Nevertheless, the presence of the magnetic field splits the energy level $J = 1$ into three different energy levels $m_J = 0, \pm 1$ such that the system turns into a *four-level system* illustrated in figure 14. This effect is

---

[1]   A linear magnetic field is not a real magnetic field since it does not satisfy the Gauss's law for magnetism.

known as **Zeeman splitting** (26, Section 7.4). Essentially, assuming a weak magnetic field[2], there will be a effective detuning $\delta_Z^{(m_J)}$ due to the **anomalous Zeeman effect** so that

$$\delta_Z^{(m_J)} = -\beta g_J m_J z, \quad \text{being} \quad \beta \equiv \frac{\mu_B B_0}{\hbar}, \tag{3.1}$$

where g_J is the *Landé factor* and μ_B is the Bohr magneton. From equation (3.1), we can see that the detuning, also called **Zeeman shift**, depends linearly on the position z so that $\delta_Z^{(m_J)} \propto z$.

Figure 14 – Zeeman splitting in 1D-MOTs
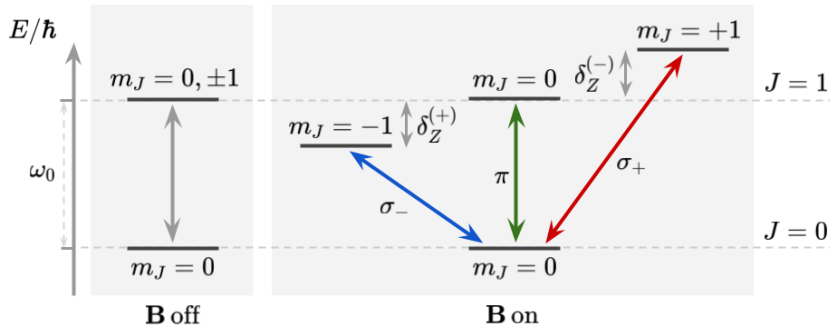
Zeeman splitting of the transition $J = 0 \rightarrow J = 1$ in 1D-MOTs. When $\mathbf{B} = 0$ ($\mathbf{B}$ off), the atomic transition $J = 0 \rightarrow J = 1$ is described by a **degenerate two-level system**. However, when $\mathbf{B} \neq 0$ ($\mathbf{B}$ on), the same atomic transition is represented by a **four-level system** in which the excited states are energetically separeted by the Zeeman shift $\delta_Z^{(\pm)}$. The energy scale was not plotted precisely to enhance the visibility.
Source: Author

### 3.1.1 Cooling and trapping effect

In this section, we shall qualitatively tackle the 1D-MOT to get a first understanding of the theory. Let us consider an arbitrary atom from an atomic cloud in a MOT. Also, let us disregard interatomic interactions. Although the momentum exchange between atoms and light are quantized, we can evaluate the atom dynamics classically by assuming a mean force $\mathbf{F}_{MOT}$, which means a **semiclassical approach**. In the general case, there is no way to obtain an analytical expression for this mean force since we have to solve the Optical Bloch equations for a four-level atom interacting with multiple fields. Nonetheless, we can obtain an analytical expression under some conditions, which shall be done in the next section 3.1.2.

---

[2] The quantity $\mu_B B$, where B is the magnetic field magnitude, must be much lower than the spin-orbit coupling energy.

The mean MOT force can be split into two components[3]: one exclusively associated with coherent transitions (absorption and *stimulated* emission); and another associated with decoherence decays (absorption and *spontaneous* emission). In weak atom-light coupling, stimulated emission is much less frequent than spontaneous emission. Therefore, $\mathbf{F}_{MOT}$ ought to be a **radiation pressure force**. Essentially, we can assume $\mathbf{F}_{MOT} = (F_+ - F_-)\mathbf{e}_z$, where $F_\pm$ is related to the interaction between atom and the $\sigma_\pm$-beam. Thus, $F_\pm$ depends on the detuning $\Delta_\pm$ such that the lower $|\Delta_\pm|$, the greater $F_\pm$. The detuning $\Delta_\pm$ can be split into three detunings (figure 15) so that $\Delta_\pm = \delta + \delta_Z^\pm + \delta_D^\pm$. These detunings are given by

- *Laser detuning $\delta = \omega - \omega_0$*: associated with the laser frequency ω and the energy difference ω_0 of the atomic transition. This detuning is the same for all transitions;

- *Doppler shift $\delta_D^{(\pm)} = \mp kv$*: associated with the atomic movement (see section 2.3.8.3);

- *Zeeman shift $\delta_Z^{(\pm)} \propto \mp z$*: associated with the Zeeman splitting. This detuning is given by the equation (3.1).

Figure 15 – Detuning in 1D-MOT
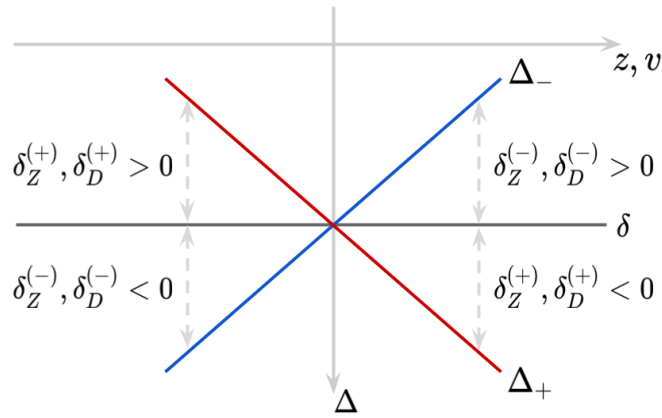
Laser detuning, Doppler shift, and Zeeman shift of a 1D-MOT in function of velocity v and position z assuming red-detuned laser beams ($\delta < 0$).
Source: Author

Both Doppler shift and Zeeman shift increase linearly with the atom velocity and atom position respectively. Assuming red-detuned laser beams ($\delta < 0$) and $v > 0$, the probability of absorbing the $\sigma_\pm$-beam decreases (increase) with v since $|\Delta_\pm|$ increases (decreases). When $v < 0$, the opposite effect occurs. Therefore, the MOT force is opposite to the velocity v ($\partial \mathbf{F}_{MOT}/\partial v < 0$) such as a friction, which is is essentially a **cooling mechanism** also known as **Doppler cooling**. The Zeeman shift behaves the same in function of z such that the MOT force is also opposite to the position ($\partial \mathbf{F}_{MOT}/\partial z < 0$), which is essentially a **trapping mechanism**.

---

[3] In section 2.3.9, we deduced both forces for the case of a two-level atom interacting with a single field.

3.1.2 MOT Force

We shall get deeper into the 1D-MOT analysis by quantifying the MOT force. As mentioned in section 3.1.1, there is no analytical expression for the MOT forces in the general case in which we take the simutaneous interaction between both laser beams and the atom into account. Although, we can obtain such analytical expression under two approximations:

- By breaking the four-level system (figure 14) into three independent two-level systems illustrated in figure 16. That is a strong assumption in which the coherence effects between the Zeeman states, such as Raman-like transitions (25, Section 9.8), are neglected;

- By assuming that the atom density operator $\hat{\rho}(\mathbf{k}, -\mathbf{k})$ related to the simultaneous interaction equals the sum of the density operators $\hat{\rho}_+(\mathbf{k})$ and $\hat{\rho}_-(-\mathbf{k})$ associated with the individual interactions, which is essentially a superposition ($\hat{\rho} = \hat{\rho}_+ + \hat{\rho}_-$). This approximation relies on the perturbation theory in first and second-order (38, Chapter 7).

Both approximations are valid in the regime of weak atom-light coupling so that the total detuning is higher than the power-broadened linewidth.

Figure 16 – Assumption of independent two-level systems
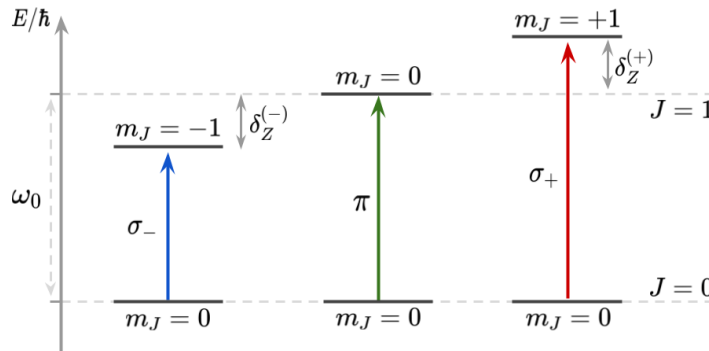
Breaking of the four-level system into three independent two-level systems.
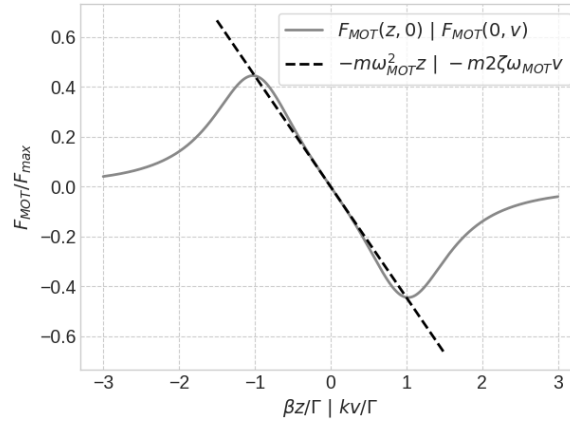Source: Author

Since there are only right-handed and left-handed polarized beams, there will only $\sigma_\pm$-transitions. Therefore, the components F_+ and F_- associated with the σ_+ and σ_- transitions respectively are independent radiation pressure forces given by (see section 2.3.9.1)

$$F_\pm(z, v) = \pm \hbar k \frac{\Gamma}{2} \frac{s_0}{1 + s_0 + 4(\Delta_\pm/\Gamma)^2},$$

(3.2)

where $\Delta_\pm = \delta + \delta_Z^{(\pm)} + \delta_D^{(\pm)}$, s_0 is the saturation parameter, and Γ is the natural linewidth[4] of the transition $J = 0 \rightarrow J = 1$. Assuming low velocities ($|kv| \ll |\delta|$) and positions close to the magnetic field centre ($|z| \ll |\delta|$), the MOT force is essentially linear with z and v as illustrated in figure 17. Hence, we can expand F_{MOT} about $z = 0$ and $v = 0$ so that

$$F_{MOT}(z, v) \simeq F_{MOT}(0, 0) + z \frac{\partial F_{MOT}}{\partial z}(0, 0) + v \frac{\partial F_{MOT}}{\partial v}(0, 0), \qquad (3.3)$$

Figure 17 – MOT force

Plotting of the MOT force F_{MOT} for $v = 0$ ($z = 0$) in function of $\beta z/\Gamma$ (kv/Γ) considering the transition $^1S_0 \rightarrow {}^1P_1$ of the ^{88}Sr for $\delta = -\Gamma$ and $s_0 = 1$. The dashed line in the graph is the MOT force assuming $|\beta z| \ll |\delta|$ ($|kv| \ll |\delta|$).
Source: Author

Rearranging the terms of equation (3.3), we obtain

$$\frac{d^2 z}{dt^2} + 2\zeta \omega_{MOT} \frac{dz}{dt} + \omega_{MOT}^2 z = 0, \qquad (3.4)$$

$$\omega_{MOT}^2 \equiv -\frac{1}{m} \frac{8\hbar k \beta g_J s_0 (\delta/\Gamma)}{[1 + s_0 + 4(\delta/\Gamma)^2]^2}, \quad \text{and} \quad \zeta \equiv \frac{k}{2\beta g_J} \omega_{MOT}, \qquad (3.5)$$

where m is the atomic mass. The quantity ω_{MOT} has unit of frequency and ζ is a dimensionless quantity. Also, ω_{MOT}^2 is a positive real value since we are assuming red-detuned lasers, which means $\delta < 0$ in equation 3.5. The equation of motion (3.4) describes a *damped harmonic oscillation* of which ω_{MOT} is the *undamped frequency* and ζ is the *damping ratio*. Hence, the atom is trapped by the restoring force $-m\omega_{MOT}^2 z$, being restrict to move in a restricted region (**trapping mechanism**). Furthermore, the atom loses energy due to the damping $2\zeta \omega_{MOT} v$, which is a **cooling mechanism**.

3.2 Three-dimensional case

---

[4]   The natural linewidth depends on the energy difference between the states, which is slightly different in each transition. However, this energy difference is much lower than $\hbar\omega_0$ such that the natural linewidth is approximately Γ.

Figure 18 – Standard 3D-MOT arrangement
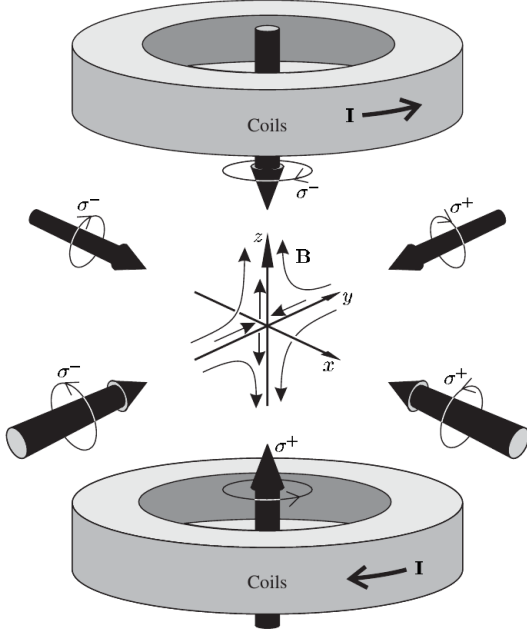
Standard arrangement of MOT composed of three orthogonal pairs of counter propagating laser beams with opposite circular polarization and coils in anti-Helmholtz configuration, which produces a magnetic quadrupole field.

Source: (25, Figure 9.9)

Let us assume the standard 3D-MOT arrangement illustrated in figure 18. An atom, free to move along all Cartesian axes, interacts with *three pairs* of counter-propagating laser beams with opposite circular polarization and a magnetic quadrupole field **B**. In a first attempt, we can naturally extend the 1D-MOT theory into a 3D theory considering that each laser beam yields a radiation pressure force given by equation (3.2). Nevertheless, the quantization axis (z-axis) must match the direction of the field **B** to proper evaluate the Zeeman shift, which implies that each laser beam polarization depends on the atomic position. This is not a concern in the 1D-MOT since the magnetic field has a fixed direction. Therefore, a theoretical description of the 3D-MOT (20) encounters considerable difficult due to the spatial-dependence of the quantization axis. Regardless the theoretical complications, the cooling and trapping effects of MOTs are widely confirmed for many alkali (39–41) and lanthanide (13–15). Also, in this thesis, we could demonstrate both effects for dysprosium and strontium atoms through a stochastic simulation. Moreover, it is possible to estimate temperature and also atomic cloud size.

3.2.1 Limit temperature in Doppler cooling

Let us consider a equilibrium atomic position close to the magnetic field centre. In this case, the Zeeman shift becomes negligible compared to the Doppler shift ($\delta_Z \ll \delta_D$) such that a defined quantization axis is no longer required. [5] Also, we suppose weak atom-light couplings in which the laser detuning are grater than the power-broadened linewidth. Thus, the interaction between each laser beam and the atom is independent and it is described by two-level dynamics. In this situation, the MOT force is given by

$$\mathbf{F}_{MOT}(\mathbf{v}) = \frac{\hbar k \Gamma s_0}{2} \sum_{n=1}^{3} \left(\frac{1}{1 + s_0 + 4[\delta - k(\mathbf{v} \cdot \mathbf{e}_n)]^2/\Gamma^2} - \frac{1}{1 + s_0 + 4[\delta + k(\mathbf{v} \cdot \mathbf{e}_n)]^2/\Gamma^2} \right) \mathbf{e}_n, \tag{3.6}$$

---

[5]   Essentially, we are proposing the treatment of a MOT as an **optical molasses**, which is a similar technique to only cool an atomic dilute gas based upon *Doppler cooling*.

where $\{\mathbf{e}_1, \mathbf{e}_2, \mathbf{e}_3\}$ is the Cartesian basis. We are assuming all laser beams with the same saturation parameter s_0, wavevector magnitude k, and detuning δ. For low velocities v such that $kv \ll \delta$, we can expand the MOT force around $\mathbf{v} = 0$ so that $\mathbf{F}_{MOT} \simeq -\gamma\mathbf{v}$,

$$\gamma = -\frac{8\hbar k^2 s_0 (\delta/\Gamma)}{[1 + s_0 + 4(\delta/\Gamma)^2]^2}.$$ (3.7)

Assuming red-detuned laser beams ($\delta < 0$), we have $\gamma > 0$ and then $\mathbf{F}_{MOT}$ describes a friction force. Hence, the velocity vanishes after a time as long as $1/\gamma$ and then the final temperature should be zero. However, the $\mathbf{F}_{MOT}$ is an average and therefore we must take its fluctuations into account. These fluctuations are associate with the Brownian atomic motion due to spontaneous emission, which yields a *heating process*. Therefore, a finite temperature is set by the balance between cooling and heating mechanisms.

Let us considering a cycle of N

3.2.2 Atomic cloud size

3.3 Narrow Line Magneto-Optical Trap

Average behaviour of the radiation pressure force

Random atoms trajectory

Defining nMOTs through the eta parameter

3.3.1 Doppler, power-broadening, and quantum regimes

3.3.2 Gravity-assisted nMOT

Recently, a two-species five-beam nMOT (42) employing gravity-assisted trapping was accomplished, bringing possibilities to elaborate nMOTs with a reduced number of beams.

4 nMOT stochastic dynamics

4.1 Markovian Evolution

4.2 Monte Carlo simulation

4.3 Data processing

5 Results

5.1 Standard nMOT arrangements

5.1.1 Dysprosium

5.1.2 Strontium

5.2 Non-standard nMOT arrangements

6 Conclusion

References

1 PETERS, A.; CHUNG, K. Y.; CHU, S. High-precision gravity measurements using atom interferometry. **Metrologia**, IOP Publishing, v. 38, n. 1, p. 25, 2001.

2 MUKAMEL, S. *et al.* Roadmap on quantum light spectroscopy. **Journal of Physics B: Atomic, Molecular and Optical Physics**, IOP Publishing, v. 53, n. 7, p. 072002, 2020.

3 CHU, S. Nobel lecture: The manipulation of neutral particles. **Reviews of Modern Physics**, APS, v. 70, n. 3, p. 685, 1998.

4 COHEN-TANNOUDJI, C. N. Nobel lecture: Manipulating atoms with photons. **Reviews of Modern Physics**, APS, v. 70, n. 3, p. 707, 1998.

5 PHILLIPS, W. D. Nobel lecture: Laser cooling and trapping of neutral atoms. **Reviews of Modern Physics**, APS, v. 70, n. 3, p. 721, 1998.

6 METCALF, H. J.; STRATEN, P. Van der. Laser cooling and trapping of neutral atoms. **The Optics Encyclopedia: Basic Foundations and Practical Applications**, Wiley Online Library, 2007.

7 LUDLOW, A. D. *et al.* Optical atomic clocks. **Reviews of Modern Physics**, APS, v. 87, n. 2, p. 637, 2015.

8 SCHNEIDER, P.-I.; SAENZ, A. Quantum computation with ultracold atoms in a driven optical lattice. **Physical Review A**, APS, v. 85, n. 5, p. 050304, 2012.

9 ZHANG, X.; YE, J. Precision measurement and frequency metrology with ultracold atoms. **National Science Review**, Oxford University Press, v. 3, n. 2, p. 189–200, 2016.

10 CORNELL, E. A.; WIEMAN, C. E. Nobel lecture: Bose-einstein condensation in a dilute gas, the first 70 years and some recent experiments. **Reviews of Modern Physics**, APS, v. 74, n. 3, p. 875, 2002.

11 KETTERLE, W. Nobel lecture: When atoms behave as waves: Bose-einstein condensation and the atom laser. **Reviews of Modern Physics**, APS, v. 74, n. 4, p. 1131, 2002.

12 KRZYSZTOF, K. *et al.* Magneto-optical trap: fundamentals and realization. **CMST**, PSNC, Poznan Supercomputing and Networking Center, n. 2, p. 115–129, 2010.

13 FRISCH, A. *et al.* Narrow-line magneto-optical trap for erbium. **Physical Review A**, APS, v. 85, n. 5, p. 051401, 2012.

14 MAIER, T. *et al.* Narrow-line magneto-optical trap for dysprosium atoms. **Optics letters**, Optical Society of America, v. 39, n. 11, p. 3138–3141, 2014.

15 MIYAZAWA, Y. *et al.* Narrow-line magneto-optical trap for europium. **Physical Review A**, APS, v. 103, n. 5, p. 053122, 2021.

16 LETT, P. D. *et al.* Observation of atoms laser cooled below the doppler limit. **Physical review letters**, APS, v. 61, n. 2, p. 169, 1988.

17 GATTOBIGIO, G. *et al.* Scaling laws for large magneto-optical traps. **Physica Scripta**, IOP Publishing, v. 81, n. 2, p. 025301, 2010.

18 LOO, F. *et al.* Investigations of a two-level atom in a magneto-optical trap using magnesium. **Journal of Optics B: Quantum and Semiclassical Optics**, IOP Publishing, v. 6, n. 1, p. 81, 2003.

19 BALYKIN, V.; MINOGIN, V.; LETOKHOV, V. Electromagnetic trapping of cold atoms. **Reports on Progress in Physics**, IOP Publishing, v. 63, n. 9, p. 1429, 2000.

20 PRUDNIKOV, O.; TAICHENACHEV, A.; YUDIN, V. Three-dimensional theory of the magneto-optical trap. **Journal of Experimental and Theoretical Physics**, Springer, v. 120, n. 4, p. 587–594, 2015.

21 CHAUDHURI, S.; ROY, S.; UNNIKRISHNAN, C. Realization of an intense cold rb atomic beam based on a two-dimensional magneto-optical trap: Experiments and comparison with simulations. **Physical Review A**, APS, v. 74, n. 2, p. 023406, 2006.

22 ATUTOV, S. *et al.* Sodium mot collection efficiency as a function of the trapping and repumping laser frequencies and intensities. **The European Physical Journal D-Atomic, Molecular, Optical and Plasma Physics**, Springer, v. 13, n. 1, p. 71–82, 2001.

23 HANLEY, R. K. *et al.* Quantitative simulation of a magneto-optical trap operating near the photon recoil limit. **Journal of Modern Optics**, Taylor & Francis, v. 65, n. 5-6, p. 667–676, 2018.

24 WEINER, J.; HO, P.-T.; DEE, K. C. **Light-matter interaction: fundamentals and applications**. [*S.l.: s.n.*]: Wiley Online Library, 2003. v. 1.

25 FOOT, C. J. *et al.* **Atomic physics**. [*S.l.: s.n.*]: Oxford University Press, 2005. v. 7.

26 STECK, D. A. Quantum and atom optics. 2007.

27 VALVERDE, C.; BASEIA, B.; BAGNATO, V. Mecanismos de alargamento de linhas espectrais atômicas. **Revista Brasileira de Ensino de Física**, SciELO Brasil, v. 38, 2016.

28 REINAUDI, G. *et al.* Strong saturation absorption imaging of dense clouds of ultracold atoms. **Optics letters**, Optical Society of America, v. 32, n. 21, p. 3143–3145, 2007.

29 SMITH, D. A. *et al.* Absorption imaging of ultracold atoms on atom chips. **Optics express**, Optical Society of America, v. 19, n. 9, p. 8471–8485, 2011.

30 SHU-BIN, Y. *et al.* Absorption spectroscopy of cold caesium atoms confined in a magneto-optical trap. **Chinese Physics**, IOP Publishing, v. 13, n. 10, p. 1669, 2004.

31 BRASIL, C. A.; FANCHINI, F. F.; NAPOLITANO, R. d. J. A simple derivation of the lindblad equation. **Revista Brasileira de Ensino de Física**, SciELO Brasil, v. 35, n. 1, p. 01–09, 2013.

32 TORREY, H. Transient nutations in nuclear magnetic resonance. **Physical Review**, APS, v. 76, n. 8, p. 1059, 1949.

33 KUHR, S. *et al.* Deterministic delivery of a single atom. **Science**, American Association for the Advancement of Science, v. 293, n. 5528, p. 278–280, 2001.

34 FUHRMANEK, A. *et al.* Imaging a single atom in a time-of-flight experiment. **New Journal of Physics**, IOP Publishing, v. 12, n. 5, p. 053028, 2010.

35 BÜCKER, R. *et al.* Single-particle-sensitive imaging of freely propagating ultracold atoms. **New Journal of Physics**, IOP Publishing, v. 11, n. 10, p. 103039, 2009.

36 PERRIN, H. Doppler cooling and magneto-optical trapping. **Part of the Les Houches lectures on laser cooling and trapping**, 2014.

37 LOFTUS, T. H. *et al.* Narrow line cooling and momentum-space crystals. **Physical Review A**, APS, v. 70, n. 6, p. 063413, 2004.

38 BERMAN, P. R.; MALINOVSKY, V. S. **Principles of laser spectroscopy and quantum optics**. [*S.l.: s.n.*]: Princeton University Press, 2011.

39 RAAB, E. L. *et al.* Trapping of neutral sodium atoms with radiation pressure. **Physical review letters**, APS, v. 59, n. 23, p. 2631, 1987.

40 KATORI, H. *et al.* Magneto-optical trapping and cooling of strontium atoms down to the photon recoil temperature. **Physical Review Letters**, APS, v. 82, n. 6, p. 1116, 1999.

41 ZACHOROWSKI, J.; PALASZ, T.; GAWLIK, W. Magneto-optical trap for rubidium atoms. **Optica Applicata**, SPIE-THE INT SOC FOR OPTICAL ENGINEERING, v. 28, p. 239–248, 1998.

42 ILZHÖFER, P. *et al.* Two-species five-beam magneto-optical trap for erbium and dysprosium. **Physical Review A**, APS, v. 97, n. 2, p. 023633, 2018.